

ANTI-NOCICEPTION INDUCED BY HIGH-INTENSITY ELECTRICAL BRAIN
STIMULATION

By

JULIETA TREJO

Presented to the Faculty of the Graduate School of
The University of Texas at Arlington in Partial Fulfillment
of the Requirements
for the Degree of

MASTER OF SCIENCE IN EXPERIMENTAL PSYCHOLOGY

THE UNIVERSITY OF TEXAS AT ARLINGTON

DECEMBER 2023

Supervising Committee:

Dr. Yuan Bo Peng, Supervising Professor
Dr. Linda Perrotti
Dr. Perry Fuchs

Copyright © by

Julieta Trejo

2023

All Rights Reserved

Acknowledgements

It is with great honor that I have the privilege to thank my mentor, Dr. Yuan Bo Peng. Dr. Peng's patience, advocacy and belief in me, and never-ending wisdom is something that I will hold dear to my heart forevermore.

A special thank you to my thesis committee members, Dr. Linda Perrotti and Dr. Perry Fuchs, for equipping me to be the best researcher that I can be through their insightful advice and support.

I would also personally like to thank Zhen Wang for his guidance and assistance, even when he is miles away. Additionally, to Dr. Linda Perrotti and her lab for allowing me to share their lab space. Specifically, to my colleague and friend, Blake Brady, for not only walking alongside me through the many trials and errors of learning a new histological procedure, but for also being the best listener and healthiest unofficial therapist.

I would like to thank my parents, sister, and nephew for being my greatest confidants, cheerleaders, and everything in between. I will be eternally thankful to my mom and dad who did not have much growing up but made sure that I had everything. It is through them that I know unwavering love, determination, and perseverance.

Finally, to the rest of my family and friends, your never-ending support is everything that I could ever ask for and more. I love you all, tenfold.

Abstract

ANTI-NOCICEPTION INDUCED BY HIGH-INTENSITY ELECTRICAL BRAIN STIMULATION

Julieta Trejo, BS

The University of Texas at Arlington, 2023

Supervising Professor: Dr. Yuan Bo Peng

A universal, and possibly one of the most frequent symptomatic motives to explore professional medical attention, is pain. Pain is defined as “an unpleasant sensory and emotional experience associated with, or resembling that associated with, actual or potential tissue damage” by The International Association for the Study of Pain. Nociceptive pain is characterized as the indication or warning of tissue damage occurring from disease or trauma. In other words, nociception is an encoder of noxious stimuli (chemical, mechanical, or thermal). Anti-nociception is the body’s sensory nervous system response to these categories of pain.

Over the years, local field potential (LFP) has grown in interest for many researchers. The LFP is known to demonstrate the activity of neurons around the recording electrode in a localized area. The LFP is a signal that displays the discourse of brain activity throughout multiple neural networks. Furthermore, the LFP can be subdivided into 5 frequency bands of delta (0.1 – 3 Hz), theta (3 – 7 Hz), alpha (7 – 12 Hz), beta (12 – 30 Hz), and gamma (30 – 100 Hz).

A diverse neuromodulatory technique, known as transcranial electrical stimulation (tES), has gained prevalence not only in the field of neuroscience, but also in other areas such as the military or in sports. This unique technique utilizes scalp electrodes that deliver weak currents to

the brain which can affect neural processing, ultimately affecting behavior. A higher intensity of stimulation is the principal application of electroconvulsive therapy (ECT). For many decades, ECT has been used as a treatment in individuals with critical mood and psychotic disorders who have shown a resistance to previous treatments used. Some of these disorders include severe depression, schizophrenia, schizoaffective disorder, catatonia, and bipolar disorder. ECT has also been revealed to be effective for chronic pain.

The **purpose** of this study is to determine the effect of ECT on LFP activities from various brain regions responding to nociceptive stimuli in anesthetized animals as well as assessing the formalin-induced behavioral activity with ECT treatment in freely-moving animals. The **hypothesis** is that ECT will suppress pain, as indicated by suppressing the LFP power by activation of the descending inhibitory system, and by reduction of formalin-behavior response. In the present study, LFPs will be recorded simultaneously from the contralateral anterior cingulate cortex (ACC), ventral tegmental area (VTA), and bilateral central amygdala (left and right CeA). In this study, there are **two specific aims**: (1) To determine the effect of ECT on the reduction of formalin-induced LFP power in anesthetized animals, and (2) to assess the formalin-induced behavioral activity with ECT treatment in freely-moving animals. This study revealed that (1) ECT has a trend of a brief suppressive effect on formalin-induced LFP power when administered after formalin injection, and (2) in behavioral testing, ECT administration produced significant pain-relief results in comparison to the control group. In **conclusion**, the results from this study demonstrates ECT stimulation yielding anti-nociceptive properties.

Table of Contents

Acknowledgements.....	
Abstract.....	
Table of Contents.....	
List of Illustrations.....	
Chapter 1.....	1
Introduction.....	1
1.1 The ACC, VTA, bilateral amygdala, and the relation to pain.....	2
1.2 The local field potential (LFP) and the relation to pain.....	5
1.3 Formalin-induced pain.....	5
1.4 Spectrum of stimulation methods.....	6
1.5 tES, ECT and the relation to pain.....	9
1.6 Specific aims.....	10
Chapter 2.....	10
Methods.....	10
2.1 Animal preparation.....	10
2.2 Electrode implantation.....	11
2.3 Module setup and LFP recording.....	12
2.4 Formalin model induction.....	13
2.5 Transcranial electrical stimulation model induction.....	13

2.6 Data analysis	15
2.7 Nissl staining.....	15
2.8 Behavioral testing.....	16
Chapter 3.....	17
Results.....	17
3.1 Histological results for the localization of electrodes	17
3.2 ECT significantly suppresses formalin behavioral response.....	18
3.3 Representative time-frequency spectrogram figures.....	20
3.3 LFP 5-minute power spectrum activities from the four designated brain regions	29
3.3.1 LFP activity from the ACC region	30
3.3.2 LFP activity from the VTA region	31
3.3.3 LFP activity from the L-CeA region	32
3.3.4 LFP activity from the R-CeA region	34
3.4 LFP 10-second power spectrum activities from all four designated brain regions.....	35
Chapter 4.....	39
Discussion.....	39
References.....	43

List of Illustrations

Figure 1. The role of the amygdala during pain inducing situations 4

Figure 2. Target of LFP recordings..... 11

Figure 3. Representation of the four-channel wireless device utilized to trace LFP signals 12

Figure 4. Procedures for anesthetized animals 14

Figure 5. Electrode tip placement 17

Figure 6. Behavioral testing in the formalin-only group versus ECT combined with formalin group 19

Figure 7. Representative raw data Spike2 time-frequency spectrogram from group B..... 21

Figure 8. Representative time-frequency spectrogram and quantified data from group A in the ACC 23

Figure 9. Representative time-frequency spectrogram and quantified data from group B in the ACC 25

Figure 10. Representative time-frequency spectrogram and quantified data from group C in the ACC 27

Figure 11. Power spectrum analysis every 5-minutes in all 3 groups 29

Figure 12. 10-second normalized power spectrum analysis for group A in the ACC 36

Figure 13. 10-second normalized power spectrum analysis for group B in the ACC 37

Figure 14. 10-second normalized power spectrum analysis for group C in the ACC 38

Table 1. Success rate for electrode implantation on-target between groups in the ACC, VTA, L-CeA, and R-CeA 18

Chapter 1

INTRODUCTION

A subjectively universal, and possibly one of the most frequent symptomatic motives to explore professional medical attention, is pain. Since 1979, pain is most internationally defined as “an unpleasant sensory and emotional experience associated with actual or potential tissue damage, or described in terms of such damage” by The International Association for the Study of Pain (IASP) (Bonica, 1979). More recently, the definition of pain has been revised by the IASP to include those who are not able to verbally describe their pain. The revised definition of pain follows as: “an unpleasant sensory and emotional experience associated with, or resembling that associated with, actual or potential tissue damage” (Raja et al., 2020). Pain is a sensory and emotional experience that is commonly and universally known and learned through experiences. This troublesome damage to tissue, more specifically the issue of chronic pain, has led to a massive amount in the monetary spending of healthcare (Loeser & Melzack, 1999).

The complex entity of pain has many characteristics and categories. The major descriptions of pain include acute pain and chronic pain. Acute pain originates by “a noxious stimulus due to an injury, a disease process, or an abnormal functioning muscle or viscera” (Russo & Brose, 1998). On the contrary, chronic pain is characterized as a pain that goes beyond six months. This type of pain is usually connected to degenerative tissue illness. One of the reasons that acute pain is short-lasting is due to its potent anti-nociceptive processes that are cohesively initiated by the noxious stimulus (Riedel et al., 2001).

Pain can be generated as receptor or non-receptor pain. Receptor pain involves a nociceptive, physiological pain such as pain from the skin, muscles, or organs. Nociceptive pain is characterized as the indication or warning of tissue damage occurring from disease or trauma

(Świeboda et al., 2013). In other words, nociception is an encoder of noxious stimuli (chemical, mechanical, or thermal). Anti-nociception is the body's sensory nervous system response to these categories of pain. Furthermore, Świeboda and colleagues (2013), classify non-receptor pain as a pathological nerve or nervous system damage. Non-receptor pain includes neuropathic pain which occurs from the nerves of the spinal cord.

1.1 The ACC, VTA, bilateral amygdala, and the relation to pain

The first area of interest, the ACC, is a part of the limbic system and contains various significant linkages to other systems and areas in the brain, such as the prefrontal cortex. More specifically, the ACC has linkages to the emotional center of the amygdala, the autonomic center of the lateral hypothalamus, the memory center of the hippocampus, and finally, the reward center of the orbitofrontal cortex and ventral striatum (Stevens et al., 2011). The dynamic system of the ACC was revealed to play a significant role in the processing of nociceptive information and pain related affective processing. More specifically, the neurons located in the ACC were revealed to be imperative in the avoidance of nociceptor stimulation (Johansen et al., 2001). Intensive behavioral studies conducted by Fuchs and colleagues (2014), further prove that the ACC contributes to pain affect processing and modulation. Demonstrating these results further, in a different study conducted by Wang and Peng (2022), the multi-linking ACC was shown to be a mediator in affective components of pain when receiving noxious stimuli via formalin injection.

Further validating the role of the ACC in the modulation of the affective component of pain, a study was conducted using L5 ligation and microinjections into the rostral anterior cingulate cortex of male rats (rACC). Results from this study reveal that in peripheral nociceptive input,

the rACC, specifically GABA_A receptors, may be involved in higher order supraspinal processing which can be utilized in the descending pain processing system (Fuchs et al., 2014; LaGraize & Fuchs, 2007). Additionally, it was revealed that when administering transcranial direct current stimulation (tDCS), there was an increase in neuronal activity in the ACC, thereby bettering the descending pain modulation system (Auvichayapat et al., 2018).

The next area of interest is the ventral tegmental area (VTA). This area is prominent in the reward process system and in motivation (Senba & Kami, 2017). The VTA contains a large number of dopaminergic neurons. More specifically, there are 55-65% of dopaminergic neurons in all VTA neurons. The rest of the neurons in the VTA are mostly composed of GABAergic inhibitory neurons (Cohen et al., 2012). The activity of VTA neurons and the extracellular levels of dopamine within areas of the forebrain are regulated from excitatory projections from the prefrontal cortex (PFC) to the VTA (Carr & Sesack, 2000). Additionally, the VTA also contributes to nociception modulation. In a study conducted by Li and colleagues (2016), direct electrical stimulation of the VTA was revealed to reduce the mechanical and thermal nociceptive thresholds caused by carrageenan injections in rats. This study points toward the idea that stimulation to the VTA could have caused an analgesic effect through descending pathways that modulate pain.

The final areas of interest are the bilateral central amygdala (left and right CeA). The GABAergic CeA is composed of the subnuclei central medial amygdala (CeM), the lateral central amygdala (CeL), and the capsular central amygdala (CeC) (Allen et al., 2021). Furthermore, the amygdala receives cortical inputs from the medial prefrontal cortex (mPFC), ACC, and insular cortex (IC), and thalamic inputs that give polymodal sensory information to the lateral amygdala (LA) and basolateral amygdala (BLA), which then adds an affective component

to the sensory information. The CeA then receives the information to further process and send to areas responsible for behavioral modulation (Kalat, 2018; Neugebauer, 2020; Thompson & Neugebauer, 2019).

Part of the limbic system, the amygdala is known to be a significant component in the regulation of fear, avoidance behavior, and during pain inducing events (Figure 1) (Goddard, 1964; Neugebauer, 2015). The amygdala also serves as an inhibitor and facilitator in nociceptive procedures and pain behavior modulation (Neugebauer et al., 2004). Furthermore, the amygdala has a region that is now known as the “nociceptive amygdala.” This region is made up by the latero-capsular division of the central nucleus of the amygdala (CeLC), and functions as an integrator of nociceptive input and input of internal and external bodily surroundings (Neugebauer et al., 2004). More specifically, in pain models, the right CeA possesses a significant pro-nociceptive role. On the contrary, a more recent and new idea in chronic and acute damage, is that the left CeA contains an anti-nociceptive role (Allen et al., 2021). This information sufficiently points toward the crucial role that the amygdala plays in nociception.

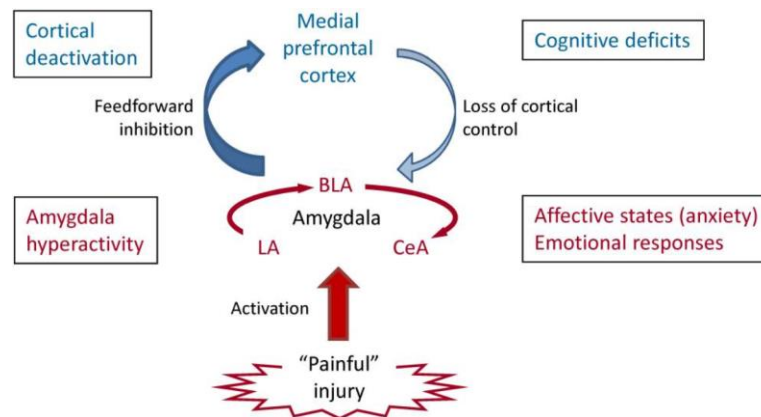


Figure 1. The role of the amygdala during pain inducing situations. Upon a painful stimulus, the LA, BLA, and CeA are hyperactivated, which adds an emotional-affective component to pain.

The BLA then deactivates the mPFC which leads to cognitive deficits (impaired decision

making). The persistence of pain is due to the continuity of amygdala hyperactivity due to the decreased mPFC output (Neugebauer, 2015).

1.2 The local field potential (LFP) and the relation to pain

Over the years, local field potential (LFP) has grown in interest for many researchers. The LFP is known to demonstrate the activity of neurons around the recording electrode in a localized area (Q. Zhang et al., 2018). The LFP is a signal that displays the discourse of brain activity throughout multiple neural networks (Halassa et al., 2016). Furthermore, the LFP can be subdivided into five frequency bands of delta (0.1 – 3 Hz), theta (3 – 7 Hz), alpha (7 – 12 Hz), beta (12 – 30 Hz), and gamma (30 – 100 Hz) (Marzbani et al., 2016). In a study conducted by Zhang and colleagues (2018), it was revealed that LFP can be utilized to measure the inception of the processing of acute nociception that corresponds with the behaviors of spinal withdrawal. Ultimately, this study demonstrates the ability to use LFP, among other factors, to detect acute pain. In a separate study conducted by Harris-Bozer and Peng (2016), the LFP was analyzed during carrageenan inflammation in freely moving rats, specifically in the ACC area. The results of this study show that when experiencing painful inflammation, there is a major change in the lowest-frequency activities in the LFP area. This study, among many others, display the phenomena of what LFP may represent during pain.

1.3 Formalin-induced pain

Formalin injections through the paw in animals has been widely utilized in pain models. The original method for this model entails for 5% formalin injection, injected subcutaneously into the dorsal surface of the forepaw in rats and cats to assess pain and analgesia with formalin-

only, and after morphine, meperidine, and PAG stimulation administration. A behavioral assessment is then utilized to test for and quantify the animal's response on a pain rating scale. Results from this test demonstrate the analgesia of morphine, meperidine, and most strikingly, PAG stimulation. In cats, it was revealed that electrical stimulation of the PAG was comparable with subjects who received morphine and meperidine, and even suggests a similarity in the mechanisms of the behavioral effects of PAG stimulation and morphine (Dubuisson & Dennis, 1977).

Formalin tests for nociception reveal that there is a first phase and a second phase of formalin response. In rats, the first phase begins immediately after injection and lasts for 5 minutes, followed by a period in which there is a decrease in response. The second phase begins around 15 – 20 minutes and lasts for an additional 40 – 60 minutes (Dubuisson & Dennis, 1977; Fuchs et al., 1996). The first phase is characterized by C-fiber activation due to head-on chemical stimulation of nociceptors, and the second phase is characterized by both an inflammatory response in the peripheral tissue and by spinal processes such as dorsal horn activity (Tjølsen et al., 1992).

1.4 Spectrum of stimulation methods

There are many types of stimulation methods that can be delivered to the brain. A diverse neuromodulatory technique, known as transcranial electrical stimulation (tES), has gained prevalence not only in the field of neuroscience, but also in other areas such as in the military and in sports. This sub-threshold unique technique utilizes scalp electrodes that deliver weak currents to the brain which can affect neural processing, ultimately affecting behavior (Berger et al., 2018). tES utilizes a low-intensity stimulation of less than 2mA (Bland & Sale, 2019). Within

tES, there are three most used noninvasive brain stimulations (NiBS): transcranial direct current stimulation (tDCS), transcranial alternating current (tACS) and transcranial random noise stimulation (tRNS) (Huang et al., 2017). In humans, these techniques are utilized for modulating behavioral functions, brain activity, cortical excitability, and the excitability of the CNS (Saiote et al., 2013; Woods et al., 2016). tDCS utilizes a constant current, while tACS and tRNS utilize oscillating currents (Saiote et al., 2013). The weak current of tDCS is most commonly used at an intensity of 1-2mA in clinical and behavioral trials (Esmailpour et al., 2018). The application of tDCS leads to the impact of motor function, learning procedures, and visual perceptual functions (Gandiga et al., 2006; Antal et al., 2004). Furthermore, the application of the sinusoidally tACS seems to interfere and synchronize cortical rhythms, and when combined with tDCS, there is an overall improvement in memory (Paulus, 2011). Finally, the application of the tRNS can work at a full range of low or high frequency from 0.1 to 640 Hz. The results of the tRNS reveal an amplification in neural excitability, and when incorporating the high-frequency band, there is an improvement in sensory, perceptual, and visual processes (Moret et al., 2019).

An additional stimulation used is transcranial magnetic stimulation (TMS), which is utilized post-stimulation for analyzing the aftermath of tES on the motor cortex (Saiote et al., 2013). Additionally, repetitive transcranial magnetic stimulation (rTMS) can “induce long-lasting, potentially therapeutic brain plasticity” (Klein et al., 2015). The next stimulation worth mentioning is known as deep brain stimulation (DBS). This invasive neuromodulatory technique directly affects the pathological neural circuits utilizing the administration of constant electricity. DBS aids in neurological and psychiatric disorders that contain flawed circuitry (Lozano et al., 2019). Additionally, DBS was revealed to be successful in alleviating unmanageable pain and chronic pain (Klein et al., 2015; Li et al., 2016). In a study conducted by Zhang and colleagues

(2022), an implantable biomedical device was created that harvests piezoelectric ultrasound energy. In rat electrophysiological experiments, this wireless-powered device yields significant results in DBS and analgesic utilizations.

In contrary to the invasive DBS technique, transcranial focused ultrasound (tFUS) is a non-invasive stimulation known to modulate brain circuits (Yu et al., 2021). tFUS is able to modulate deep brain structures through the use of its transducers that consist of piezoelectric elements that create pulses of ultrasonic waves (Badran et al., 2020). In a study conducted by Zhang and colleagues (2022), results reveal that when the periaqueductal gray (PAG) area is stimulated by tFUS, an analgesic effect occurs. More specifically, results reveal that the nociceptive input created by formalin can be suppressed through the tFUS stimulation to the PAG.

tES at a higher intensity is similar to ECT, although in contrast to the relatively weak tDCS and tACS which is commonly delivered at an intensity of less than 2mA and produces no seizure, and barely any stimulation to the scalp, the seizure-inducing electroconvulsive therapy (ECT) can be delivered at an amplitude range of 70mA to a shocking 900mA in human patients (Peterchev et al., 2011). In rat models, ECT is most delivered at an amplitude range between 50mA and 100mA (Busnello et al., 2008; Jansson et al., 2008; Jansson et al., 2009). In clinical studies, ECT works in the brain by delivering an electrical charge through scalp electrodes, and in rat models, the charge is delivered through clips attached to both ears. Researchers theorize that the stimulation of ECT generates a variety of neurophysiological and neurochemical shifts in the brain. These shifts include a change in the permeability of the blood-brain barrier, functional connectivity, gene expression, and changes in neurochemicals (Singh & Kar, 2017).

1.5 tES, ECT and the relation to pain

Regarding pain, the direct current of tDCS in fibromyalgia syndrome (FMS) revealed to be successful in pain measures. In a study conducted by Antal and colleagues (2008), cathodal tDCS in the primary somatosensory cortex (S1) was revealed to greatly decrease pain perception. Contrarily, there has not been much research on the effects of tACS for pain management (Perrey et al., 2019).

For many decades, ECT has been used as a treatment in individuals with critical mood and psychotic disorders who have shown a resistance to previous treatments used (Espinoza & Kellner, 2022). Some of these disorders include severe depression, schizophrenia, schizoaffective disorder, catatonia, and bipolar disorder (Salik & Raman, 2022). ECT has also been revealed to be effective for chronic pain with depression (Suzuki et al., 2009). In a special case, ECT was shown to alleviate neuropathic pain. In a 32-year-old male patient with chronic pain for 10 years, a significant improvement was reported after ECT administration in his depression and pain for two months (Abdi et al., 2004). In a separate study, repeated ECT sessions revealed an improvement in chronic regional pain syndrome (CRPS) with depression in a 48-year-old woman (Suzuki et al., 2009). In a chronic pain study not associated with depression, Usui and colleagues (2006), utilized ECT administration to analyze whether severe fibromyalgia pain could be alleviated. The results from this study reveal that not only was pain severity significantly lower post ECT, but there was also an improvement in thalamic blood flow after ECT administration. In a separate study, Senapati and colleagues (2005), found that inserting a bipolar stimulating electrode into the ACC region of the male rat induces a short-term dorsal horn response to mechanical stimuli. These studies point toward the notion that electrical stimulation could prove to be an efficacious treatment in pain.

1.6 Specific aims

The **purpose** of this study is to determine the effect of ECT on LFP activities from various brain regions responding to nociceptive stimuli in anesthetized animals as well as assessing the formalin-induced behavioral activity with ECT treatment in freely-moving animals. The **hypothesis** is that ECT will suppress pain, as indicated by suppressing the LFP power by activation of the descending inhibitory system, and by reduction of formalin-behavior response. In the present study, LFPs will be recorded simultaneously from the contralateral anterior cingulate cortex (ACC), ventral tegmental area (VTA), and bilateral central amygdala (left and right CeA). In this study, there are **two specific aims**: (1) To determine the effect of ECT on the reduction of formalin-induced LFP power in anesthetized animals, and (2) to assess the formalin-induced behavioral activity with ECT treatment in freely-moving animals.

Chapter 2

METHODS

2.1 Animal preparation

A total of 32 male Sprague Dawley rats with a ranging weight between 318 and 444g were used in this study. The appropriate food and water were available to the animals, and housing consisted of cages in a 12/12h light/dark cycle. The Institutional Animal Care and Use Committees (IACUC) of the University of Texas at Arlington authorized all procedures.

2.2 Electrode implantation

All rats were placed on a stereotaxic frame under induction at 3% isoflurane inhaled anesthesia for surgical procedures. After the surgical procedure, the animals were then maintained at 1.5% isoflurane inhaled anesthesia. Four 0.010in electrodes, from Plastics One Inc. 81MS3031SPCE, were separately implanted into four regions of the brain: right ACC at 0 mm posterior to bregma, 0.70 mm lateral to the right, 3.20 mm deep; right VTA at 4.80 mm posterior to bregma, 0.90 mm lateral to the right, 8.35 mm deep; and left and right CeA at 2.04 mm posterior to bregma, 4.00 mm lateral to the left and right, 8.00 mm deep (Paxinos & Watson, 1997). An illustration of the targeted brain areas are shown in Figure 2. Two screws were placed under the skull, one screw on the upper left region of the skull and the other on the upper right region of the skull, connecting to a cable as ground and reference. To stabilize the four electrodes and screws onto the skull, dental cement was then used.

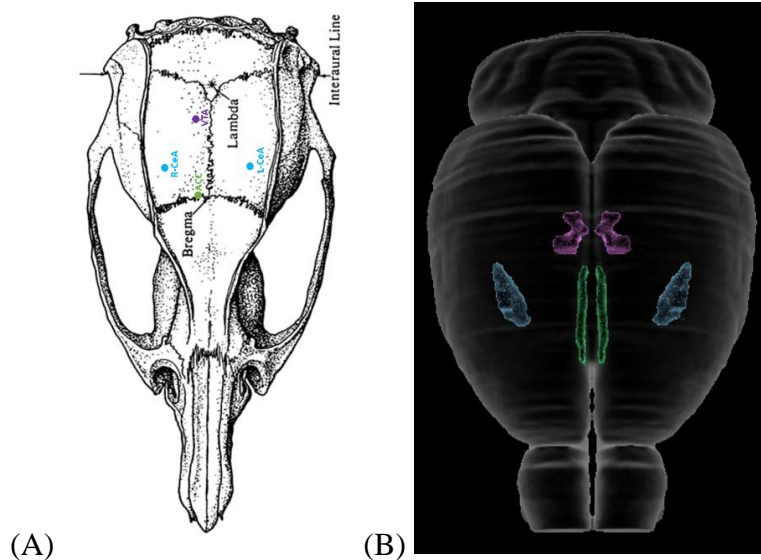


Figure 2. Target of LFP recordings. (A) Atlas image that represents the right ACC (green), right VTA (purple), and bilateral CeA (blue). (B) 3D imaging of coordinating brain regions. Green represents the ACC, purple represents the VTA, and blue represents the bilateral CeA.

2.3 Module setup and LFP recording

To record LFP signals from the brain, a wireless module designed by SiChuan NeoSource BioTektronics Limited was used, which connects to the four electrodes and screw cable. To convey the signals from the wireless module onto the recording software, a USB dongle was placed into the USB port of the laptop (Figure 3).

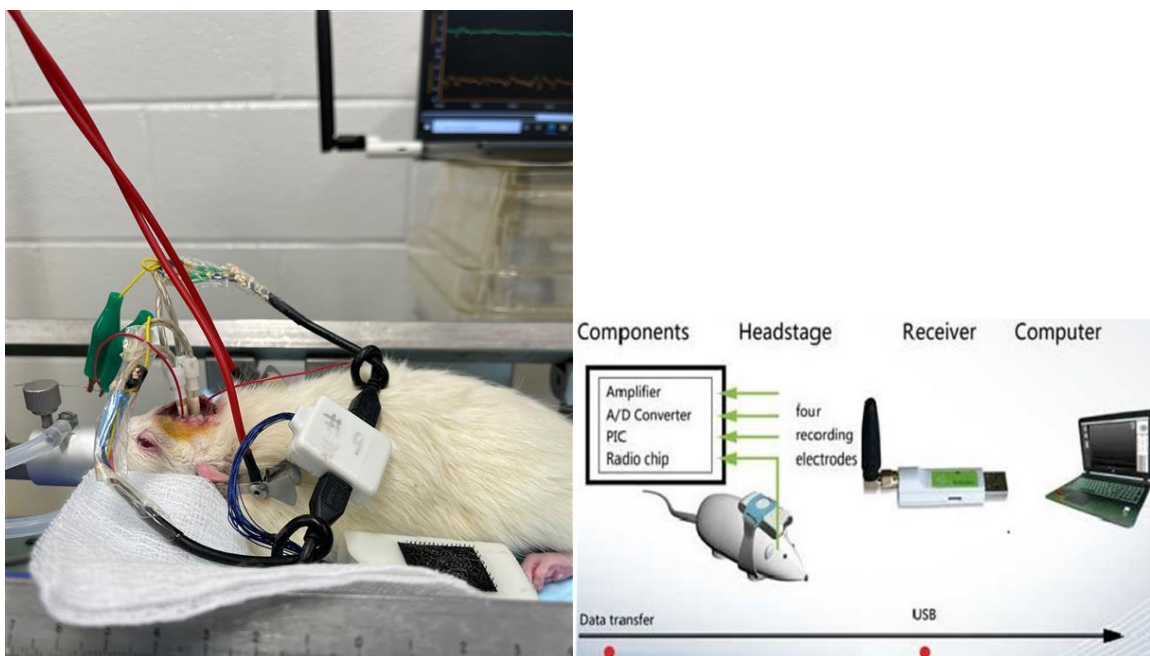


Figure 3. Representation of the four-channel wireless device utilized to trace LFP signals.

Channeled wire cables connect to the coordinating electrode. The module is then connected to the coordinating channeled wire cable. A USB dongle is then paired to the computer to track the LFP activities and coordinating channels/brain regions.

2.4 Formalin model induction

All rats had a 10-minute baseline LFP recording prior to any procedure. In the control condition ($n = 10$), after baseline, 50 μ l 3% formalin was injected subcutaneously into the plantar side of the left hind paw. Continuously, the LFP recording continued for an additional 60 minutes.

2.5 Transcranial electrical stimulation model induction

ECT unit (57800 by Ugo Basile, Italy) was utilized for the stimulation. The LFP signal was recorded for a baseline of 10 minutes under 1.5% isoflurane inhaled anesthesia. The unit was then clipped on to the left and right ear of the anesthetized rat. In the first experimental condition ($n = 12$), following the baseline recording, a 3% formalin injection was administered followed by a 20-minute LFP recording. Subsequently, the first stimulation parameter was delivered three times at 50 pulses/s, 0.7ms, 5mA for 2-seconds, each stimulation given 10-15s apart. Following the stimulation, LFP was recorded for 10-minutes. This sequence was repeated two more times with the same parameters, although the mA increased to 20mA and then 50mA for the last set of stimulations. The recording module was disconnected prior to the stimulation, and then immediately reconnected after the 3-time stimulation was completed.

In the second experimental condition ($n = 10$), the LFP signal baseline recording remained the same at 10 minutes under 1.5% isoflurane inhaled anesthesia. This time, the stimulations were administered immediately after baseline recording. The ECT parameters for the stimulations remained the same as they did for the first experimental condition. Thereafter, 10-minutes after the completion of all stimulations, a 3% formalin was then injected to the left hind paw of the rat. LFP recording continued for 60-minutes (Figure 4).

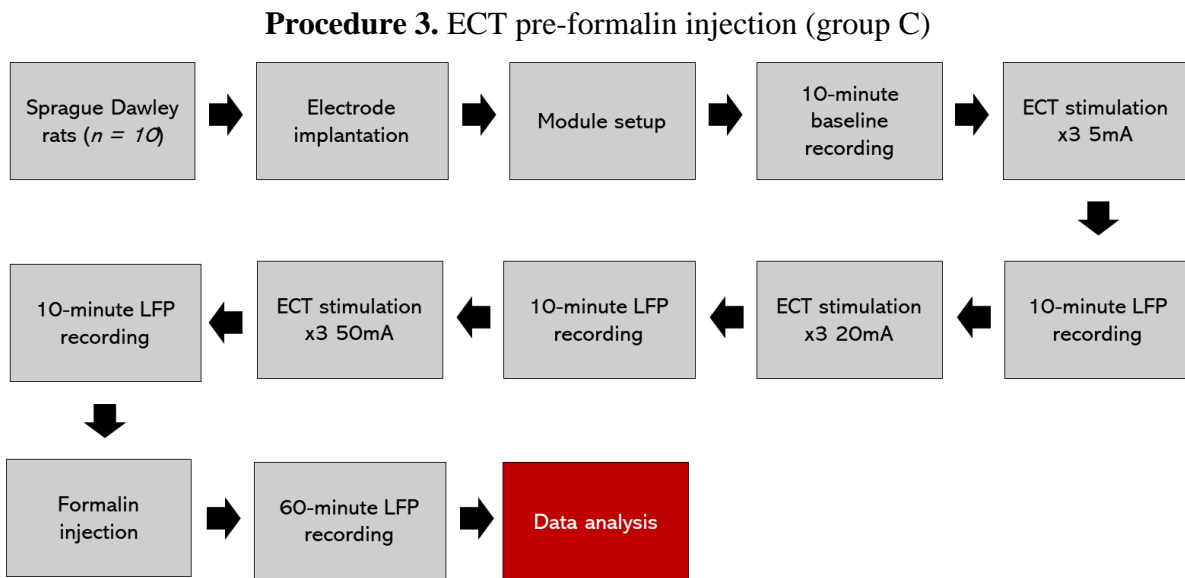
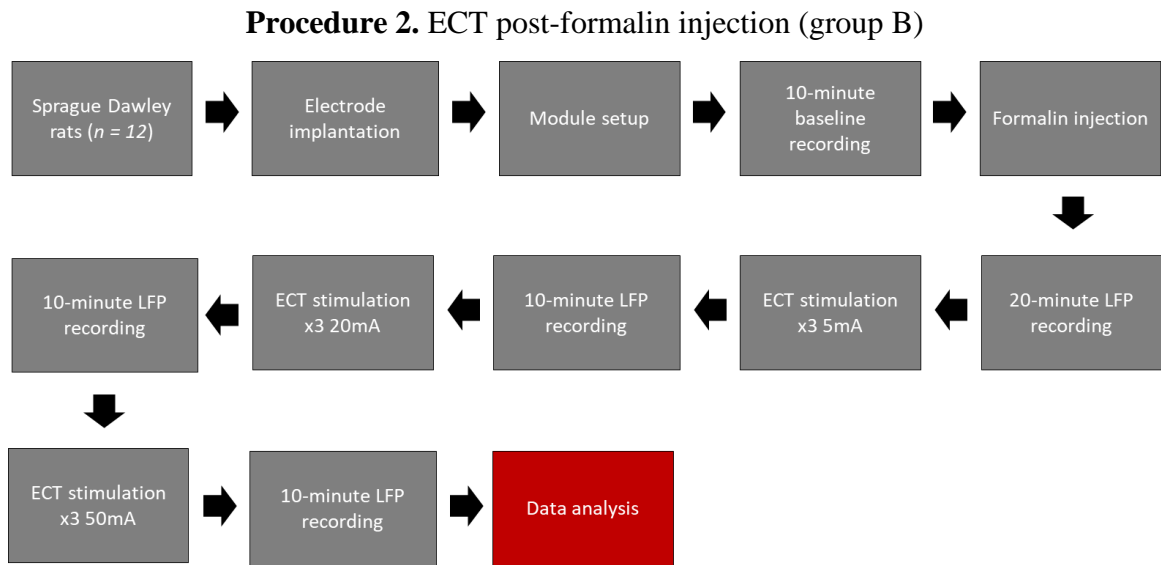
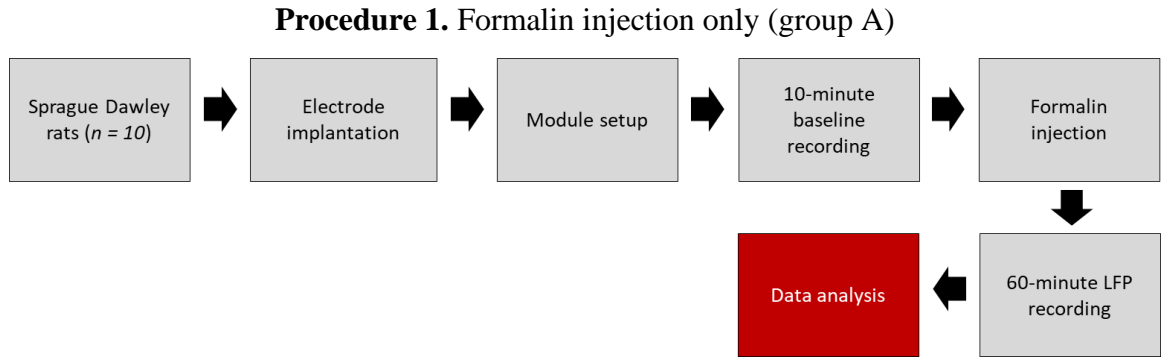


Figure 4. Procedures for anesthetized animals

2.6 Data analysis

For the data analysis, the software fast Fourier transform (FFT) in MATLAB was first analyzed from the raw data of LFPs recorded from the recording module in all four brain regions. In MATLAB, the power frequency was calculated for every 10 seconds and averaged depending on the duration. The power of the five frequency bands of delta (0.1-3 Hz), theta (3-7 Hz), alpha (7-12 Hz), beta (12-30 Hz), and gamma (30-100 Hz) was normalized by baseline average power. Next, the raw data was imported into Spike2 to analyze the data in time-frequency spectrogram and waveform graphs. Additionally, SPSS was utilized to test for statistical significance. More specifically, to determine the effect of ECT on the reduction of formalin-induced LFP power in anesthetized animals, a mixed-design analysis of variance (ANOVA) with Fisher's Least Significant Difference (LSD) post-hoc testing was conducted, and significance determined at $p < .05$ level. By using this testing, we can compare the difference of formalin and ECT effects in the LFP in the four designated brain regions (right ACC, right VTA, bilateral CeA) in the anesthetized group.

2.7 Nissl staining

To verify that electrode placement was inserted into the correct corresponding brain regions, a Nissl histological staining was conducted post-mortem. Each rat brain was mounted on a LEICA 2000R sliding microtome and sliced into 80- μ m coronal sections. The brain slices were immediately mounted with PBS solution onto a glass slide and allowed to dry for a minimum of 48hrs. Thereafter, each slide was stained using a thionin solution of .5g thionin, 500ml distilled water, and .5ml acetic acid. Once dried, the electrode lesions were cross verified through two knowledgeable researchers.

2.8 Behavioral testing

In 12 male Sprague Dawley freely-moving rats ($N = 12$) with a ranging weight between 333 and 364g, behavioral testing was conducted. In the control condition ($n = 6$), 50 μ l of 3% formalin was injected into the left hind paw. The rat was then immediately transferred to a large clear box to observe the behavior using the software DOSBox version 19.03 to determine the number of times the animal displayed specific pain-related behaviors such as “paw down,” “paw up,” and “paw licking,” with the corresponding keyboard keys of “J,” “K,” and “L.”

In one experimental condition ($n = 3$), 50 μ l of 3% formalin was injected into the left hind paw and then immediately given three ECT stimulations at 50 pulses/s, 0.7ms, 50mA for 2-seconds, each stimulation given 10-15s apart. During the procedure, the animal was kept under 2% isoflurane inhaled anesthesia. Following completion of the formalin injection and ECT stimulation, the rat was immediately transferred to a large clear box to observe the rat’s behavior.

In the next experimental condition ($n = 3$), the parameters remained the same, only this time, the set of three ECT stimulations were administered first, immediately followed by the formalin injection. Concluding behavioral testing, a repeated measures analysis of variance (ANOVA) was utilized to analyze the mean pain scores in animals who received ECT versus those with a pure formalin-only response. There were no significant differences between the two experimental conditions, so they were later merged to the “ECT + Formalin” group (Figure 6).

Chapter 3

RESULTS

3.1 Histological results for the localization of electrodes

A total of 32 rats have been used for the following three groups. (1) Group A ($n = 10$), formalin injection only, no electrode implantation or ECT was delivered. (2) Group B ($n = 12$), formalin injection followed by ECT stimulation. (3) Group C ($n = 10$), ECT stimulation followed by formalin injection. Concluding histology, the tip of the electrode was labeled and verified by two independent observers (Figure 5). If the electrode tip was within LFP's 1mm range, the data was included. In some groups, data was required to be excluded due to the tip of the electrode outside of the intended target range (Table 1).

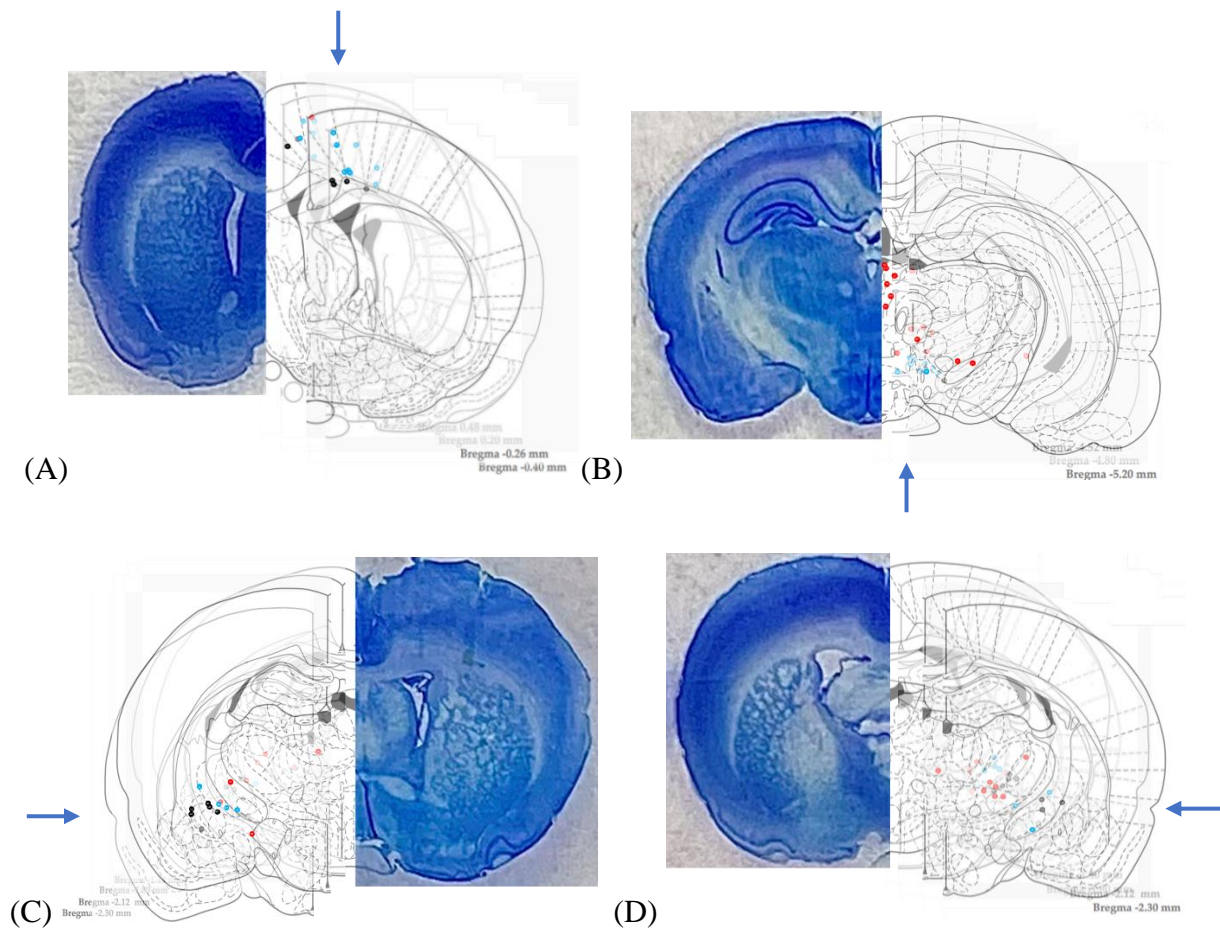


Figure 5. Electrode tip placement as indicated using Paxinos and Watson’s Rat Brain Atlas (Paxinos & Watson, 1997) and a visual representation of corresponding Nissl-stained brain slice. (A) Representative ACC region, (B) VTA, (C) left CeA, (D) and right CeA. Black dots represent electrodes on-target, blue dots represent electrodes within 1mm range, and red dots represent electrodes off-target.

	ACC	VTA	L-CeA	R-CeA
Group A	5/10	5/10	4/10	3/10
Group B	6/12	5/12	6/12	9/12
Group C	8/10	0/10	7/10	3/10

Table 1. Success rate for electrode implantation on-target between groups in the ACC, VTA, left CeA (L-CeA), and right CeA (R-CeA). Group A represents formalin-only ($n = 10$), group B represents formalin followed by ECT ($n = 12$), and group C represents ECT followed by formalin ($n = 10$).

3.2 ECT significantly suppresses formalin behavioral response

After conducting a repeated measures analysis of variance (ANOVA), results reveal a main effect of groups, $F(11, 110) = 3.833, p < .001, \eta_p^2 = .277$, suggesting that are significant differences between the formalin-only group ($M = 1.013, SE = .066$) and the ECT combined with formalin group ($M = .722, SE = .066$). The pain score trend demonstrates a significant decrease

of formalin-induced pain in the ECT condition starting at the 30-minute time point and ending at the 55-minute time point ($p < .05$) (Figure 6).

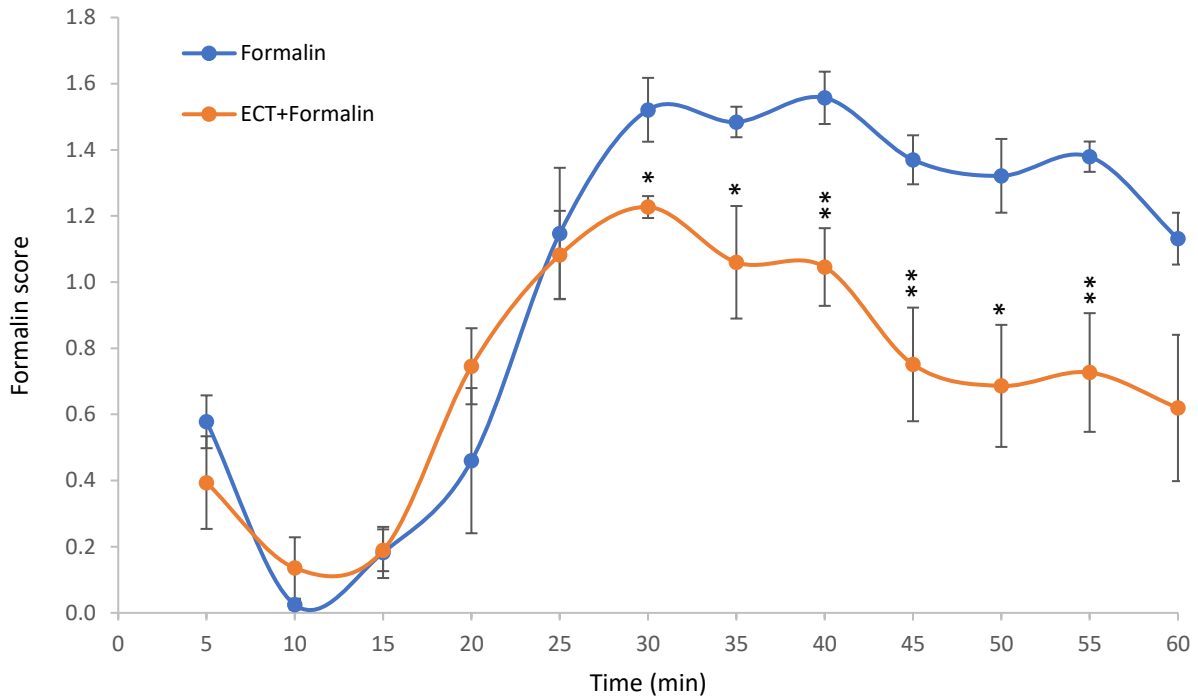
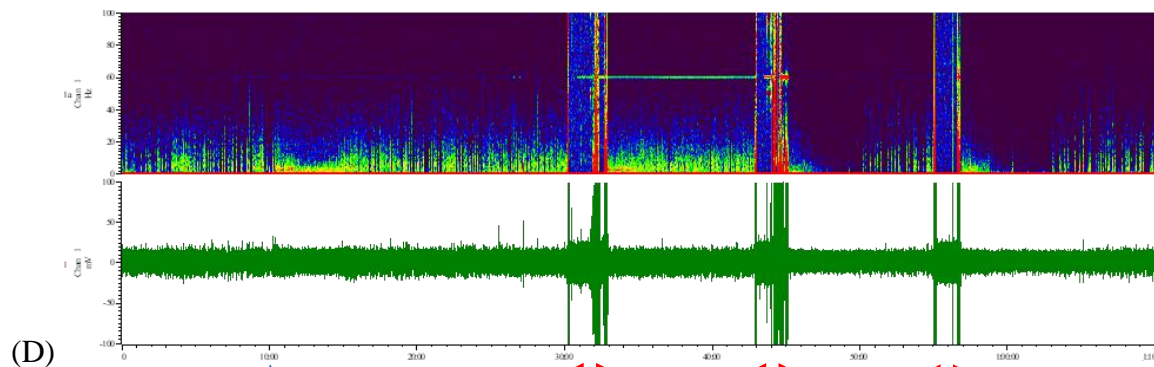
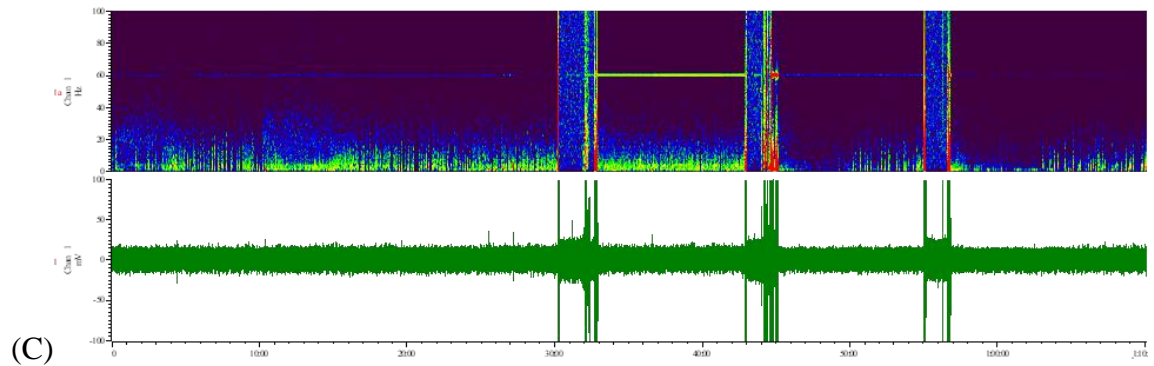
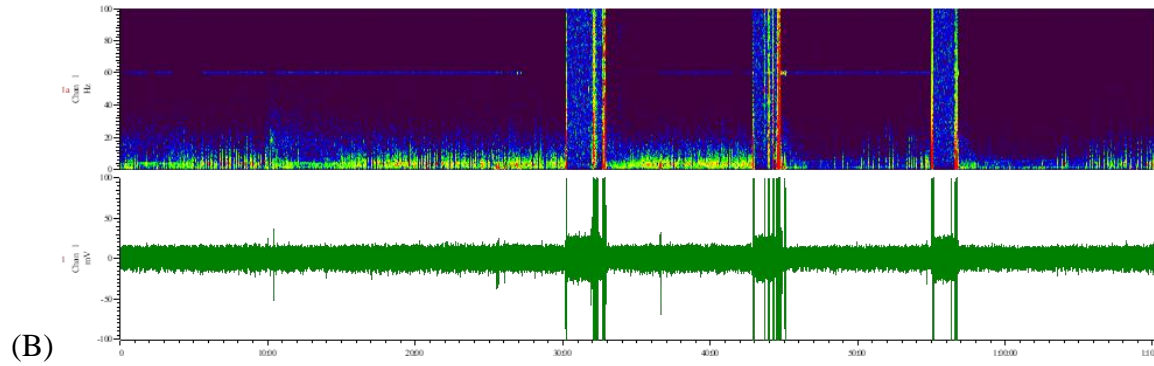
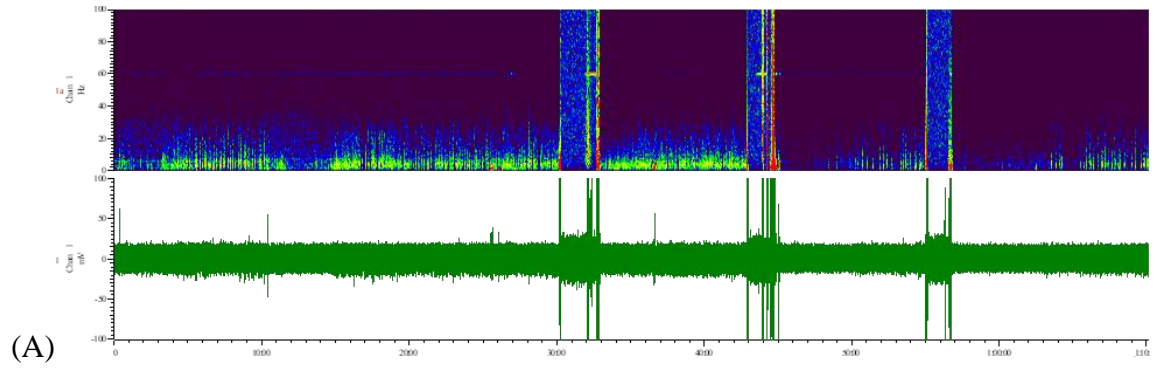


Figure 6. Behavioral testing in the formalin-only group ($n = 6$) versus ECT combined with formalin group ($n = 6$) during each 5-minute test interval. The pain score trend reveals a significant decrease when ECT is administered in comparison to the formalin-only group. Results reveal a significant difference between the 30 to 55min time points between groups. This behavioral testing data demonstrates the analgesic effect ECT may evoke. ‘*’ represents $p < .05$, ‘**’ represents $p < .01$, ‘***’ represents $p < .001$.

3.3 Representative time-frequency spectrogram figures

In the following figures, we demonstrate the representative raw traces from the LFP recordings (Figures 7, 8, 9, 10). Starting with the representation of a full recording in all four brain regions for the same subject in the formalin followed by ECT administration condition (group B) (Figure 7). Next, the formalin-only condition (group A) is demonstrated in time-frequency spectrogram and in power spectrum form for the ACC region in one subject (Figure 8). An increase of LFP power can be observed in this trace. Following, the formalin followed by ECT administration condition (group B) is also represented in time-frequency spectrogram and in power spectrum form in the ACC region of one rat (Figure 9). A brief inhibition after ECT stimulation is noticed in this trace. Finally, we also demonstrate the representative trace and power spectrum data for ECT administration followed by formalin condition (group C) (Figure 10).



↑ Formalin

↔ Disconnect module, stimulate at 5mA 2s x3, then reconnect module

↔ Disconnect module, stimulate at 20mA 2s x3, then reconnect module

↔ Disconnect module, stimulate at 50mA 2s x3, then reconnect module

Figure 7. Representative raw data Spike2 time-frequency spectrogram from subject B4 from group B (formalin followed by ECT administration). (A) Represents the ACC region, (B) VTA, (C) L-CeA, (D) R-CeA. The top portion of each figure indicates the time-frequency spectrogram, while the bottom half indicates the raw trace waveform. The y-axis represents the frequency power intensity, and the x-axis represents time. The blue arrow represents the formalin injection received after the baseline recording at 10min. The red arrows represent the location where the recording module was disconnected prior to each set of stimulations and then immediately reconnected after the stimulation period concluded. A reduction of LFP power was observed after the set of 20mA stimulations, at approximately 45-50min, and again after the 50mA set of stimulations at approximately 55-60min.

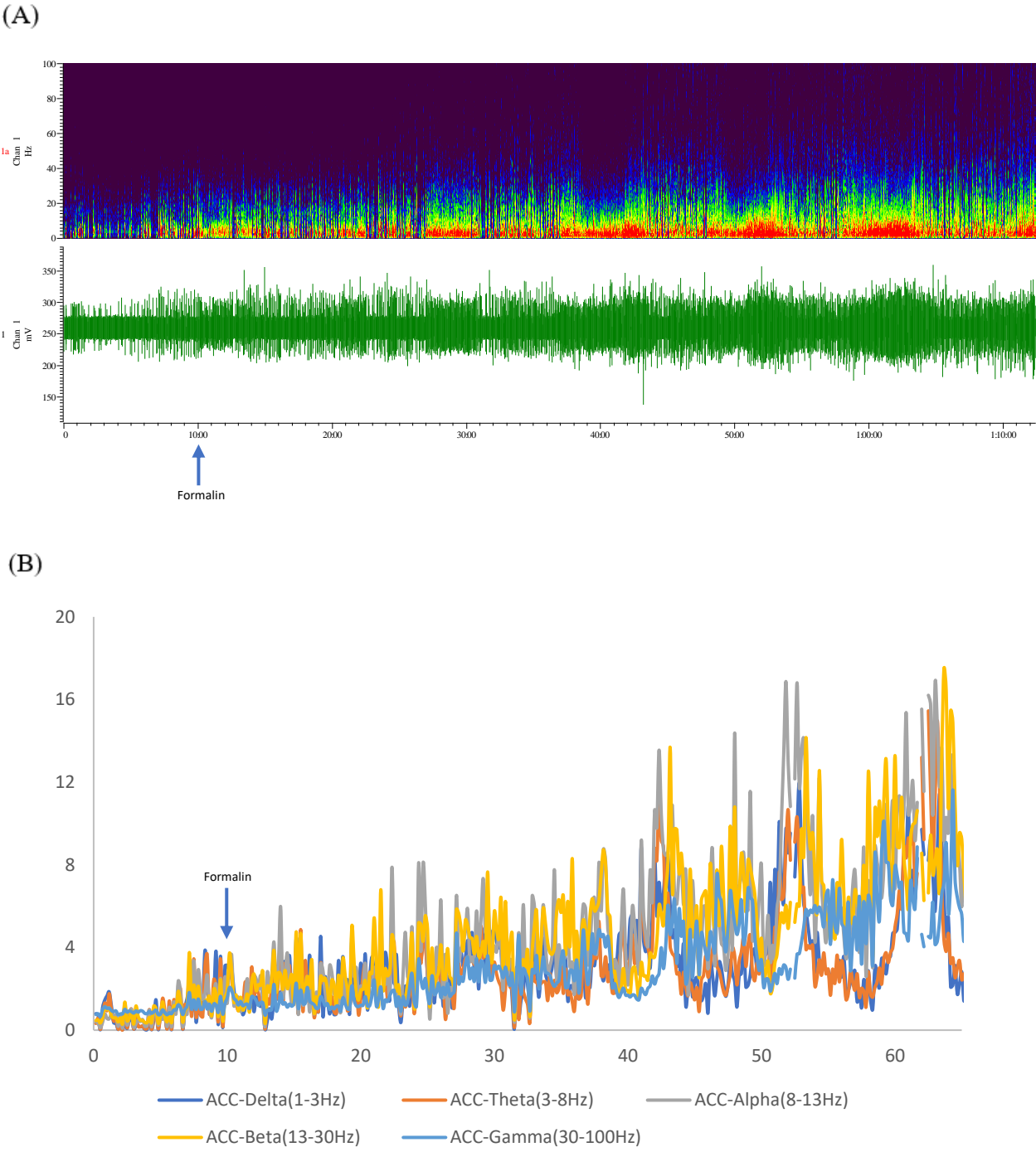


Figure 8. Representative time-frequency spectrogram and quantified data from subject A7 from group A (formalin-only) in the ACC. (A) Represents the raw data Spike2 time-frequency spectrogram. Specifically, the top portion indicates the time-frequency spectrogram, while the bottom half indicates the raw trace waveform. The y-axis represents the frequency power intensity, and the x-axis represents time. The blue arrow represents the formalin injection

received after the baseline recording at 10min. (B) The bottom graph represents the quantified power spectrum data of all 5 frequency bands (delta, theta, alpha, beta, gamma), with the y-axis representing the frequency power intensity, and the x-axis representing time. An increase of LFP power was observed after formalin injection.

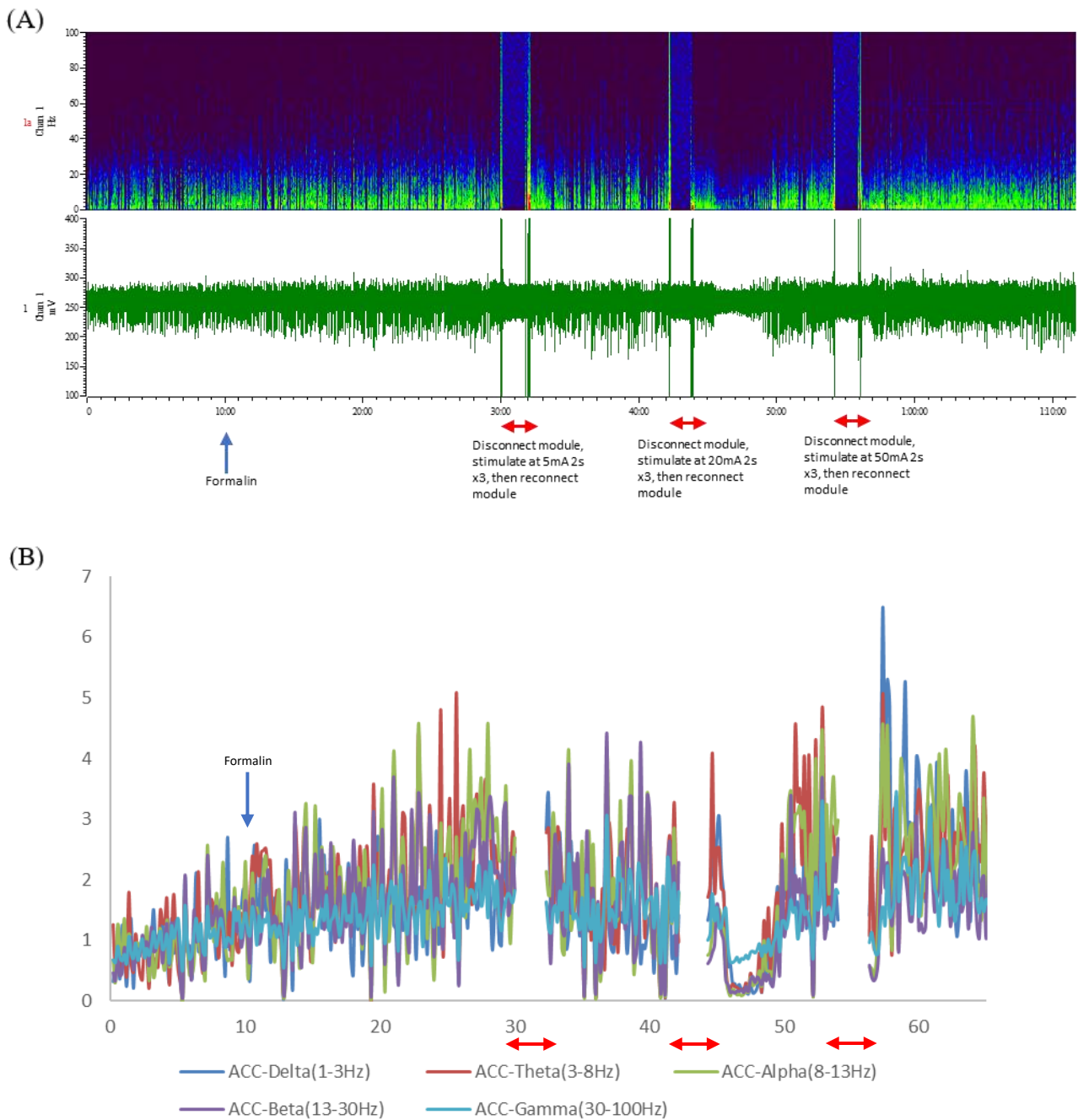
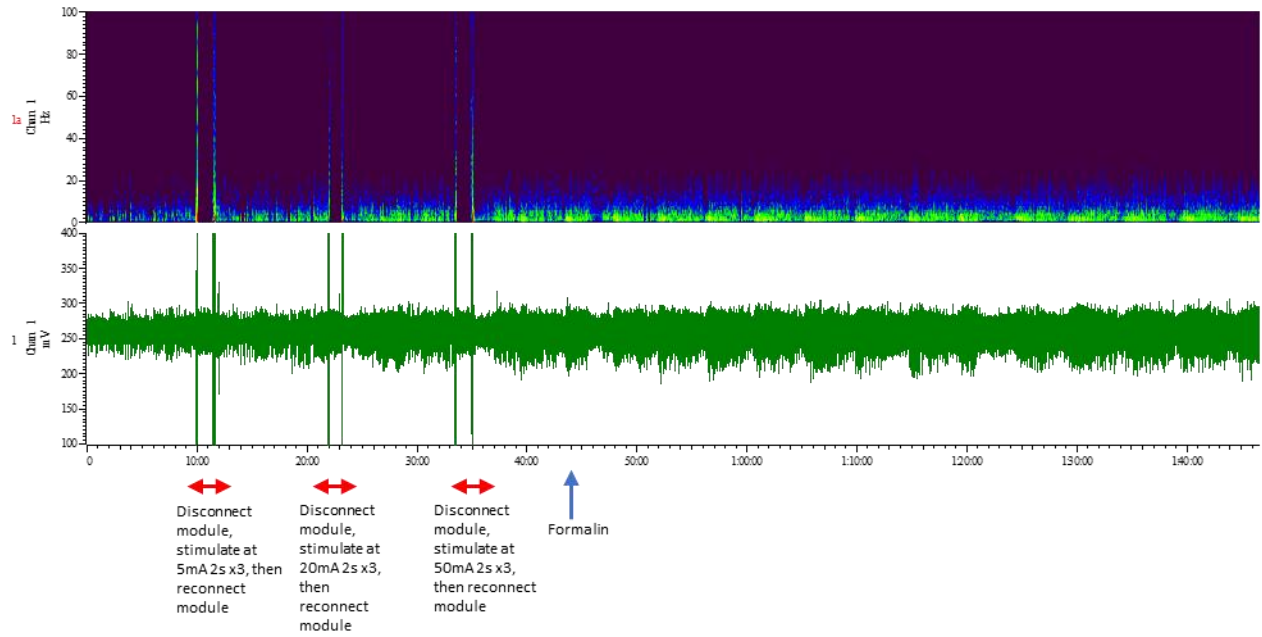


Figure 9. Representative time-frequency spectrogram and quantified data from subject B8 from group B (formalin followed by ECT administration) in the ACC. (A) Represents the raw data Spike2 time-frequency spectrogram. Specifically, the top portion indicates the power spectrogram, while the bottom half indicates the raw trace waveform. The y-axis represents the frequency power intensity, and the x-axis represents time. The blue arrow represents the formalin

injection received after the baseline recording at 10min. The red arrows represent the location where the recording module was disconnected prior to each set of stimulations and then immediately reconnected after the stimulation period concluded. (B) The bottom graph represents the quantified power spectrum data of all 5 frequency bands (delta, theta, alpha, beta, gamma), with the y-axis representing the frequency power intensity, and the x-axis representing time. An increase of power was observed post-formalin injection, followed by a brief of LFP power, most noticeably after the set of 20mA stimulation.

(A)



(B)

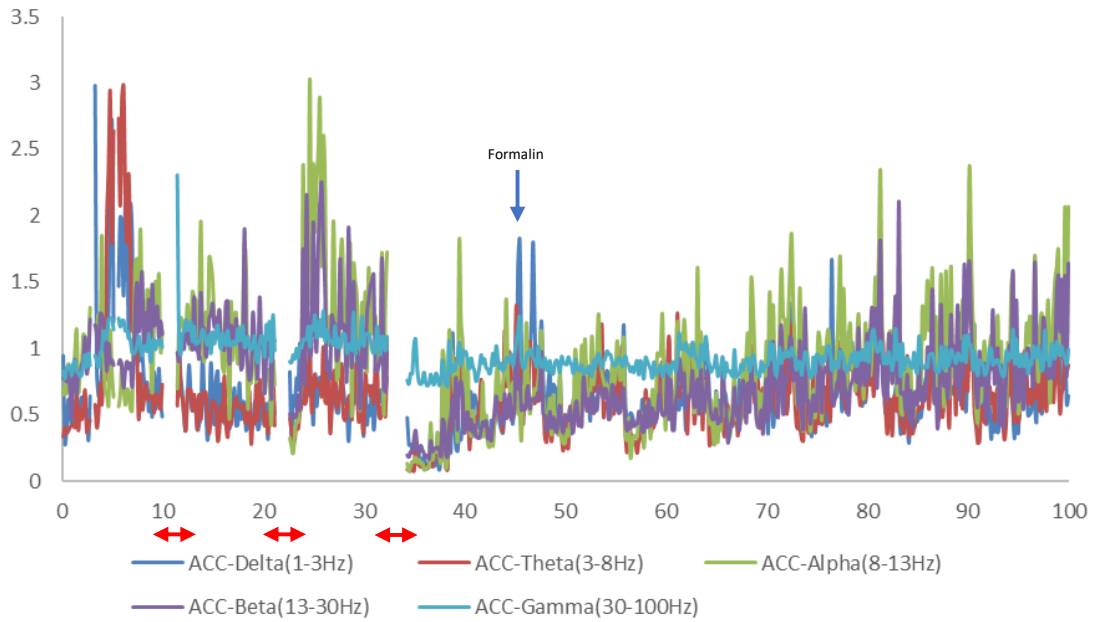


Figure 10. Representative time-frequency spectrogram and quantified data from subject C3 from group C (ECT administration followed by formalin) in the ACC. (A) Represents the raw data

Spike2 time-frequency spectrogram. Specifically, the top portion indicates the power spectrogram, while the bottom half indicates the raw trace waveform. The y-axis represents the frequency power intensity, and the x-axis represents time. After the 10min baseline, the red arrows represent the location where the recording module was disconnected prior to each set of stimulations and then immediately reconnected after the stimulation period concluded. The blue arrow represents the formalin injection received after the stimulations concluded. (B) The bottom graph represents the quantified power spectrum data of all 5 frequency bands (delta, theta, alpha, beta, gamma), with the y-axis representing the frequency power intensity, and the x-axis representing time.

3.3 LFP 5-minute power spectrum activities from the four designated brain regions

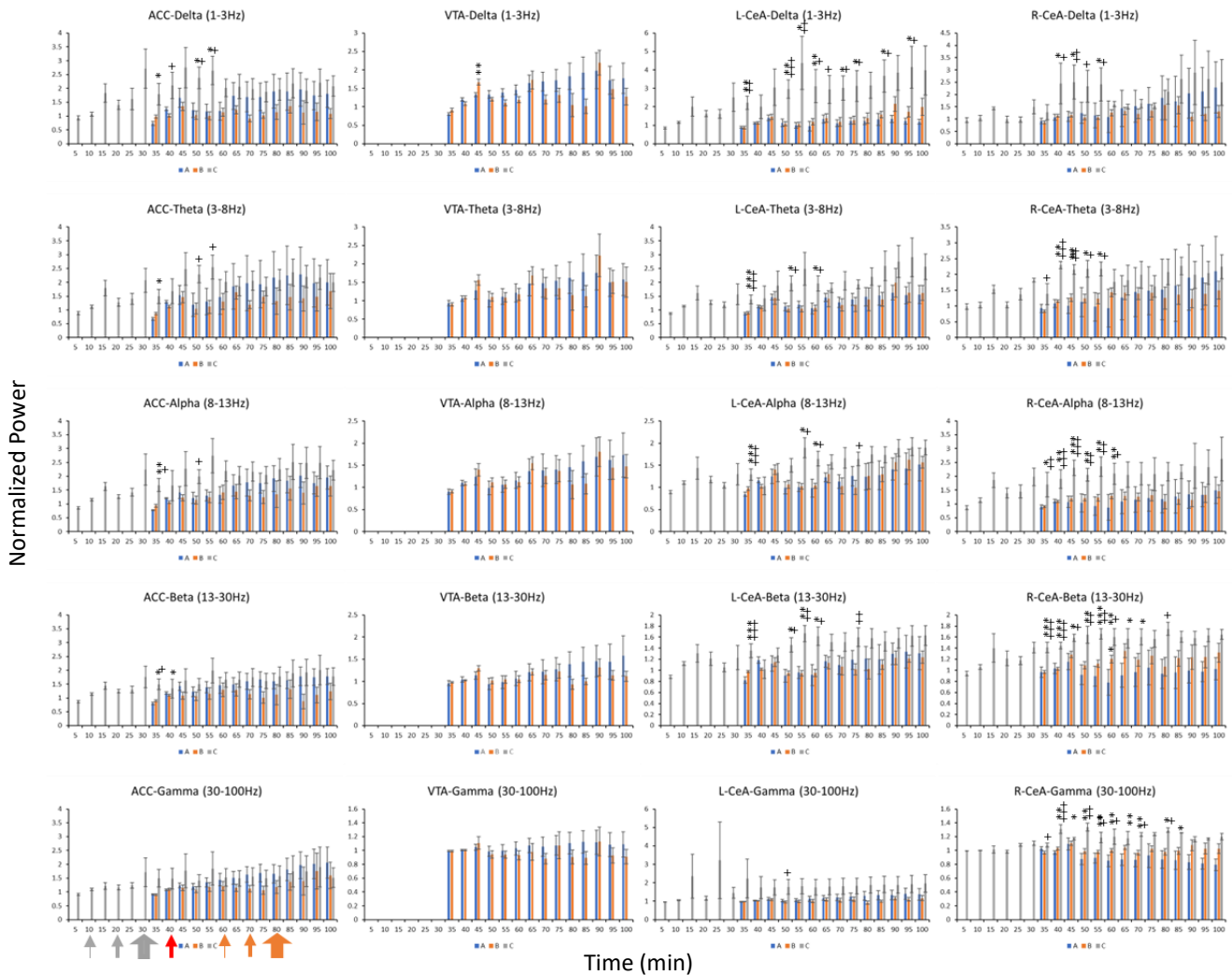


Figure 11. Power spectrum analysis every 5-minutes in all 3 groups: formalin-only, formalin followed by ECT administration, ECT administration followed by formalin administration (groups A – blue bar, B – orange bar, and C – grey bar, respectively) in the ACC ($n = 5$, group A; $n = 6$, group B; $n = 8$, group C), VTA ($n = 5$, group A; $n = 5$, group B; $n = 0$, group C), left CeA ($n = 4$, group A; $n = 6$, group B; $n = 7$, group C), and right CeA ($n = 3$, group A; $n = 9$, group B; $n = 3$, group C). Note: red arrows indicate formalin injection whereas orange and grey arrows indicate ECT administration. The thickness of the arrows represents each ECT

stimulation intensity, starting with the thin arrows depicting the weakest stimulation. ‘*’ indicates significant difference between groups A and B, or group A and C, depending on the location, ‘+’ indicates significant differences between groups B and C. ‘*’ indicates $p < .05$, ‘**’ indicates $p < .01$, ‘***’ indicates $p < .001$, and is the same for the symbol ‘+.’

3.3.1 LFP activity from the ACC region

The results using a mixed-design analysis of variance (ANOVA) with Fisher’s Least Significant Difference (LSD) post hoc testing demonstrated that there was no main effect of groups at the delta band, $F(26, 182) = 1.026, p = .436, \eta_p^2 = .128$, suggesting that there are no significant differences in the ACC delta LFP power between group A ($M = 1.543, SE = .357$), group B ($M = 1.100, SE = .357$), or group C ($M = 2.001, SE = .302$). Results reveal that there was no main effect of groups at the theta band, $F(26, 195) = .990, p = .483, \eta_p^2 = .117$, between group A ($M = 1.708, SE = .440$), group B ($M = 1.329, SE = .401$), or group C ($M = 1.882, SE = .371$). There was no main effect at the alpha band, $F(26, 195) = .807, p = .735, \eta_p^2 = .097$, between group A ($M = 1.565, SE = .387$), group B ($M = 1.332, SE = .353$), or group C ($M = 2.068, SE = .327$). There was also no main effect at the beta band, $F(26, 195) = 1.079, p = .369, \eta_p^2 = .126$, between group A ($M = 1.484, SE = .327$), group B ($M = 1.120, SE = .299$), or group C ($M = 1.687, SE = .276$). Finally, at the gamma band, there was no main effect of groups, $F(26, 156) = 1.071, p = .381, \eta_p^2 = .152$, between group A ($M = 1.540, SE = .404$), group B ($M = 1.232, SE = .369$), or group C ($M = 1.636, SE = .341$).

LFP power in the ACC reveals significance in the delta, theta, alpha, and beta bands for the first 25min in groups A and B, and 55min in group C, but no significance was found in the gamma band (Figure 11). Specifically, at the delta band, groups A and C were significant at 5-

10min in group A, and immediately after receiving the last set of simulations at 35-40min in group C ($p < .05$). In groups A and C, and B and C, significance was found after formalin injection at 20-25min in groups A and B, and after formalin injection at 50-55min in group C ($p < .05$). At the theta band, groups A and C were significant at 5min in group A, and 35min in group C ($p < .05$). In groups B and C, significance was found 10min after formalin injection at 20-25min in group B, and immediately after formalin injection at 50-55min in group C ($p < .05$). At the alpha band, groups A and C were significant at 5min in group A and immediately after the last set of stimulations at 35min in group C ($p < .05$). In groups B and C, significance was also found at 5min in group B and 35min in group C ($p < .05$). Finally, in groups B and C, significance was found 10min after formalin injection at 20min in group B, and immediately after formalin injection at 50min in group C ($p < .05$). At the beta band, groups A and C, and B and C were significant at 5-10min in groups A and B, and after the last set of stimulations at 35-40min in group C ($p < .05$). Ultimately, there were no significant differences observed in the gamma band.

3.3.2 LFP activity from the VTA region

In the VTA, there was a main effect of groups at the delta band, $F(13, 104) = 2.416$, $p = .007$, $\eta_p^2 = 2.32$, suggesting that are significant differences in the VTA delta LFP power between group A ($M = 1.554$, $SE = .180$) and group B ($M = 1.317$, $SE = .180$). Results reveal that there was no main effect of groups at the theta band, $F(13, 104) = 1.014$, $p = .443$, $\eta_p^2 = .113$, between group A ($M = 1.384$, $SE = .247$) or group B ($M = 1.343$, $SE = .247$). There was no main effect at the alpha band, $F(13, 104) = .738$, $p = .722$, $\eta_p^2 = .084$, between group A ($M = 1.333$, $SE = .200$) or group B ($M = 1.332$, $SE = .353$). There was also no main effect at the beta band, $F(13,$

104) = 1.463, $p = .144$, $\eta_p^2 = .155$, between group A ($M = 1.223$, $SE = .156$) or group B ($M = 1.107$, $SE = .156$). Finally, at the gamma band, there was no main effect of groups, $F(13, 104) = .974$, $p = .481$, $\eta_p^2 = .109$, between group A ($M = 1.056$, $SE = .098$) or group B ($M = .973$, $SE = .098$).

LFP power in the VTA reveals significance in the delta band (Figure 11). Specifically, between groups A and B, significance was found 5min after formalin injection, at the 15min mark ($p < .05$). However, no other significant changes were found in the remaining frequency bands of theta, alpha, beta, and gamma.

3.3.3 LFP activity from the L-CeA region

In the L-CeA region, results demonstrated that there was no main effect of groups at the delta band, $F(26, 156) = .780$, $p = .767$, $\eta_p^2 = .115$, suggesting that there are no significant differences in the L-CeA delta LFP power between group A ($M = 1.173$, $SE = .368$), group B ($M = 1.389$, $SE = .300$), or group C ($M = 2.655$, $SE = .329$). Results reveal that there was no main effect of groups at the theta band, $F(26, 156) = .771$, $p = .779$, $\eta_p^2 = .114$, between group A ($M = 1.332$, $SE = .366$), group B ($M = 1.312$, $SE = .299$), or group C ($M = 2.115$, $SE = .328$). There was no main effect at the alpha band, $F(26, 156) = 1.063$, $p = .392$, $\eta_p^2 = .150$, between group A ($M = 1.193$, $SE = .179$), group B ($M = 1.226$, $SE = .146$), or group C ($M = 1.597$, $SE = .160$). There was also no main effect at the beta band, $F(26, 156) = 1.361$, $p = .128$, $\eta_p^2 = .185$, between group A ($M = 1.121$, $SE = .122$), group B ($M = 1.073$, $SE = .100$), or group C ($M = 1.453$, $SE = .110$). Finally, at the gamma band, there was no main effect of groups, $F(26, 156) = 1.071$, p

= .381, $\eta_p^2 = .152$, between group A ($M = 1.193$, $SE = .439$), group B ($M = 1.047$, $SE = .359$), or group C ($M = 1.986$, $SE = .393$).

LFP power in the L-CeA reveals significance in the frequency bands of delta, theta, alpha, beta, and gamma among groups A, B and C (Figure 11). Specifically, at the delta band, groups A and C, and B and C, were significant at 5min in groups A and B, and after the last set of stimulations at 35min in group C ($p < .05$). In groups A and C, significance was found in group A 10min after formalin injection at 20-30min, and immediately after formalin injection at 50-60min in group C ($p < .05$). In groups B and C, significance was found 10min after formalin injection at 20min, and after the second set of stimulations delivered at 20mA at 45min in group B, and immediately after formalin injection at 50-75min in group C ($p < .05$). In groups A and C, and B and C, significance was found at the 55 and 65min mark in groups A and B, and 85 and 95min marks in group C ($p < .05$). At the theta band, groups A and C were significant at 5-10min in group A and at 35-40min in group C ($p < .05$). In groups B and C, significance was found at 5min in group B, and 35min in group C ($p < .05$). In groups A and C, and B and C, significance was found at the 20 and 30min mark in groups A and B, and 50 and 60min mark in group C ($p < .05$). At the alpha band, groups A and C were significant at 5-10min in group A, and 35-40min in group C ($p < .05$). Significance was also revealed in groups B and C at 5min in group B, and 35min in group C ($p < .05$). In groups A and C, and B and C, significance was found at the 25-30min mark in groups A and B, and 55-60min mark in group C ($p < .05$). Furthermore, significance was found in groups B and C at 45min in group A, and 75min in group C ($p < .05$). At the beta band, groups A and C, and B and C were significant at 5min in group A and B, and 35min in group C ($p < .05$). Significance was also revealed in groups A and C, and B and C at 20-30min in groups A and B, and 50-60min in group C ($p < .05$). In groups B and C,

significance was found at 45min in group B and 75min in group C ($p < .05$). At the gamma band, significance was found in group B and C at 20min in group B, and 50min in group C.

3.3.4 LFP activity from the R-CeA region

In the R-CeA, there was no main effect of groups at the delta band, $F(26, 143) = 1.396$, $p = .113$, $\eta_p^2 = .202$, suggesting that there are no significant differences in the R-CeA delta LFP power between group A ($M = 1.516$, $SE = .378$), group B ($M = 1.164$, $SE = .232$), or group C ($M = 2.144$, $SE = .378$). Results reveal that there was no main effect of groups at the theta band, $F(26, 156) = .668$, $p = .886$, $\eta_p^2 = .100$, between group A ($M = 1.379$, $SE = .337$), group B ($M = 1.295$, $SE = .195$), or group C ($M = 1.999$, $SE = .337$). Results also demonstrated that there was no main effect of groups in the alpha band, $F(26, 156) = .337$, $p = .999$, $\eta_p^2 = .053$, suggesting that there are no significant differences in the R-CeA alpha LFP power between group A ($M = 1.142$, $SE = .273$), group B ($M = 1.214$, $SE = .158$), or group C ($M = 2.165$, $SE = .273$). Additionally, there was not a main effect of groups at the beta band, $F(26, 156) = .499$, $p = .980$, $\eta_p^2 = .077$, between group A ($M = .969$, $SE = .151$), group B ($M = 1.184$, $SE = .087$), or group C ($M = 1.594$, $SE = .151$). Finally, there was also no main effect of groups at the gamma band, $F(26, 143) = 1.148$, $p = .297$, $\eta_p^2 = .173$, between group A ($M = .895$, $SE = .050$), group B ($M = 1.016$, $SE = .029$), or group C ($M = 1.215$, $SE = .062$).

LFP power in the R-CeA reveals significance in the frequency bands of delta, theta, alpha, beta, and gamma among groups A, B and C (Figure 11). At the delta band, in groups A and C, significance was found immediately after formalin injection at 10-15min in group A, and 40-45min in group C ($p < .05$). In groups B and C, significance was also revealed after formalin

injection 10-25min in group B, and 40-55min in group C ($p < .05$). In group B and C, significance was found at 25min in group B and 55min in group C, immediately after the first set of stimulations given in the B group ($p < .05$). At the theta band, significance was found in group B and C at 5-25min in group B, and 35-55min in group C. Significance was also found in group A and C at 10-25min in group A (post formalin injection), and prior-to and after formalin injection at 40-55min in group C ($p < .05$). At the alpha band, significance was found in groups A and C, and B and C, at 5-30min in groups A and B, and 35-60min in group C ($p < .05$). At the beta band, significance was found in group A and C at 5-40min in group A, and 35-70min in group C ($p < .05$). In group B and C, significance was found at 5-30min in group A, and 35-60min in group C ($p < .05$). Significance was found in group A and B 20min after receiving formalin injection, and immediately after receiving the first set of stimulations at 30min ($p < .05$). Significance was also found in group B and C, after receiving the second set of stimulations at 50min in group B, and at 80min in group C, approximately 30min after formalin injection ($p < .05$). At the gamma band, in group B and C, significance was found at 5-10min and 20-30min in group B, and 35-40min and 50-60min in group C ($p < .05$). Significance was also found in group A and C at 5-35min in group A, and 40-70min in group C. In group B and C, significance was revealed at 40min and 50min in group B, and 70min and 80min in group C ($p < .05$). Finally, significance was revealed in group A and C at 55min in group A, and 85min in group C ($p < .05$).

3.4 LFP 10-second power spectrum activities from all four designated brain regions

The power spectrum 10-second analyses (Figures 12, 13, 14) demonstrate the quantified LFP power in graph form. In the formalin-only condition (group A), an increase of LFP power

was observed post-formalin injection in all four designated brain regions (ACC, VTA, L-CeA, and R-CeA), further supporting the noxious effect of formalin (Figure 12). In the condition of formalin injection followed by ECT administration (group B), the data not only demonstrates the noxious escalating effect formalin possesses on LFP power, but this data also demonstrates the suppression of formalin-induced LFP power after receiving ECT stimulation in all four designated brain regions (Figure 13). However, we found that ECT does not exert long-lasting effects, but rather exhibits a brief suppressive effect. Although formalin injection followed by ECT administration (group B) revealed a trend of brief inhibition of formalin-induced activity in all four brain regions, ECT administration followed by formalin (group C) demonstrates a less inhibitory effect (Figure 14).

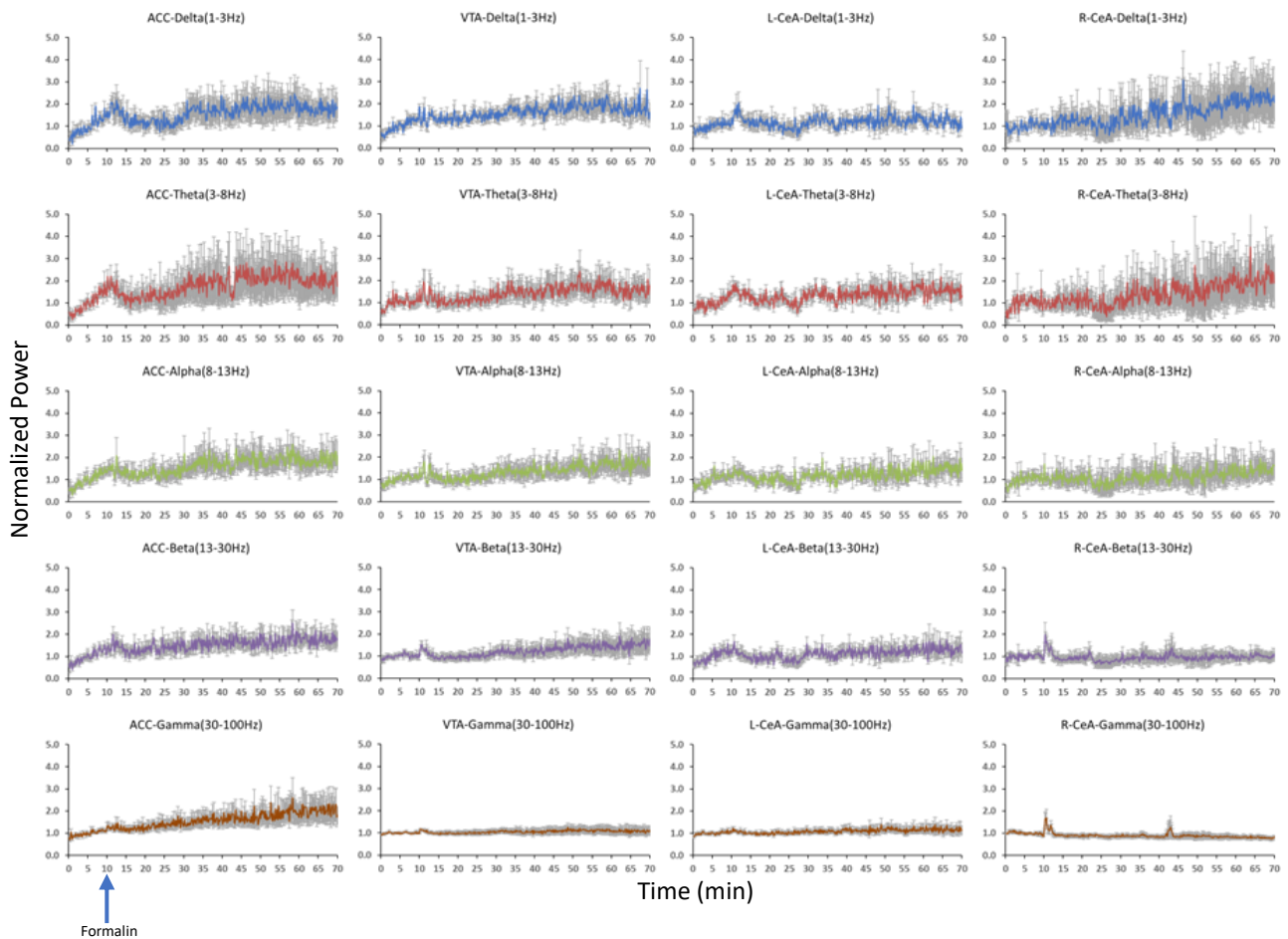


Figure 12. 10-second normalized power spectrum analysis for group A (formalin-only) in the ACC ($n = 5$), VTA ($n = 5$), left CeA ($n = 4$), and right CeA ($n = 3$). The y-axis represents the LFP normalized power ratio, while the x-axis represents time. An increase of power is observed post-formalin injection in all four brain regions.

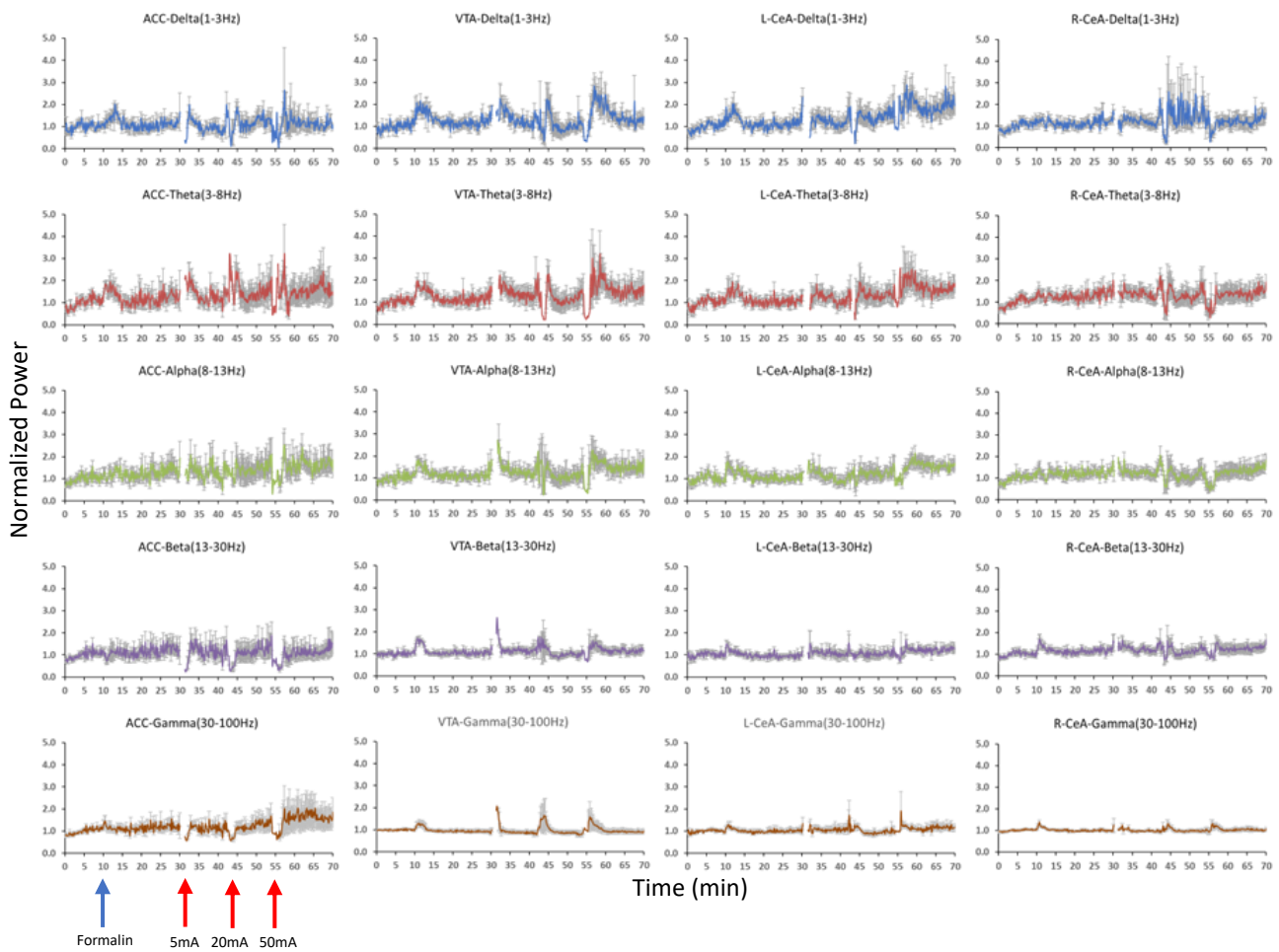


Figure 13. 10-second normalized power spectrum analysis for group B (formalin followed by ECT administration) in the ACC ($n = 6$), VTA ($n = 5$), left CeA ($n = 6$), and right CeA ($n = 9$).

The y-axis represents the LFP normalized power ratio, while the x-axis represents time. An

increase of power is observed post-formalin injection in all four brain regions, followed by a brief suppression of power after ECT stimulation.

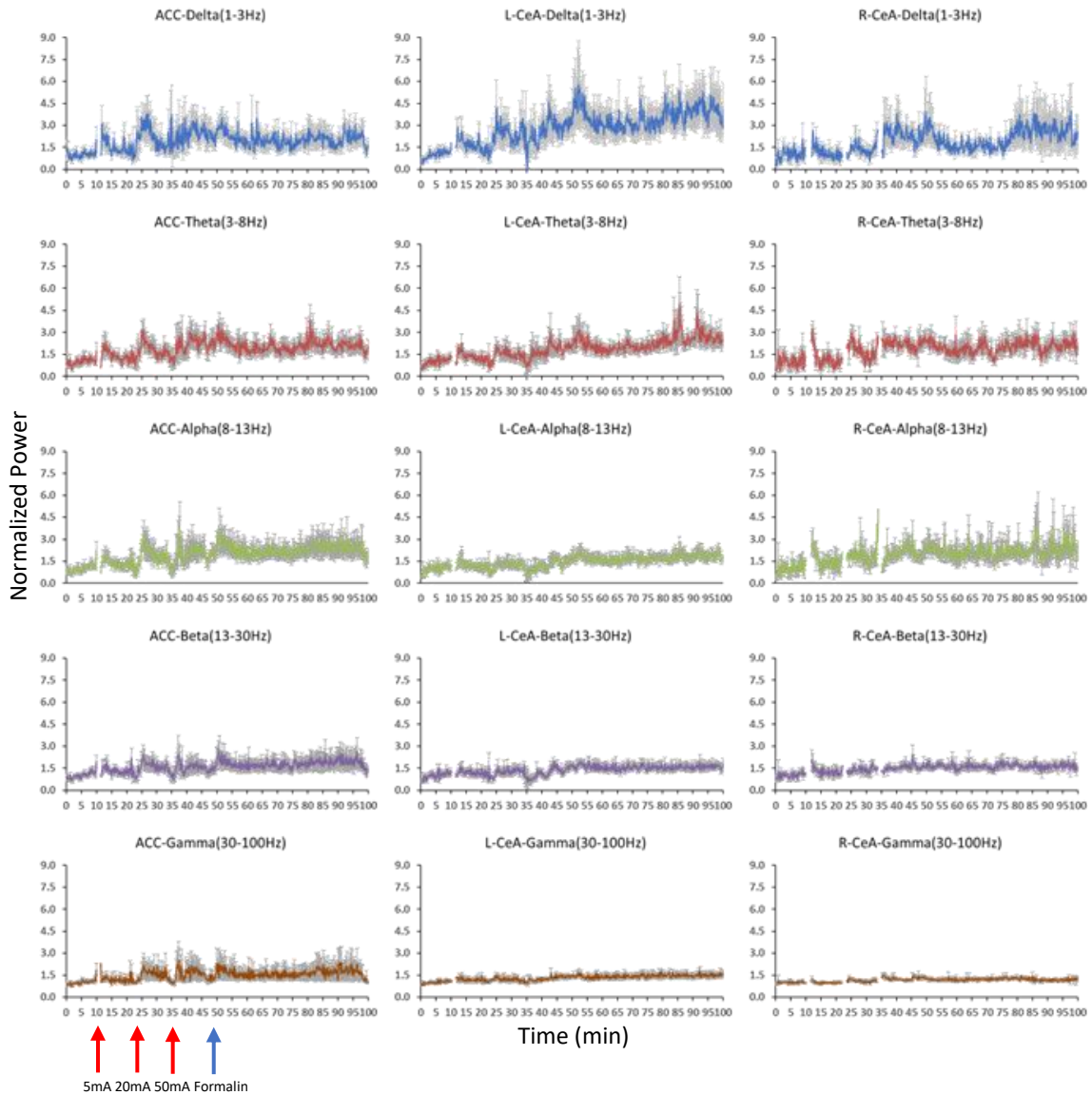


Figure 14. 10-second normalized power spectrum analysis for group C (ECT administration followed by formalin) in the ACC ($n = 8$), VTA ($n = 0$), left CeA ($n = 7$), and right CeA ($n = 3$). The y-axis represents the LFP normalized power ratio, while the x-axis represents time. A brief

increase of power is observed post-ECT stimulation, followed by an increase of power post-formalin injection in all four brain regions.

Chapter 4

DISCUSSION

The purpose of this study was to determine the effect of ECT on LFP activities from various brain regions responding to nociceptive stimuli in anesthetized animals as well as assessing the formalin-induced behavioral activity with ECT treatment in freely-moving animals. We hypothesized that ECT will suppress pain, as indicated by suppressing the LFP power by activation of the descending inhibitory system, and by reduction of formalin-behavior response. To test this hypothesis, LFPs were recorded simultaneously from the contralateral anterior cingulate cortex (ACC), ventral tegmental area (VTA), and bilateral central amygdala (left and right CeA). Animals were randomized into one of three groups: formalin-only (group A), formalin followed by ECT administration (group B), and ECT administration followed by formalin (group C). Behavioral testing was conducted in animals with formalin-only, and in combination of both formalin and ECT. There were two specific aims: (1) To determine the effect of ECT on the reduction of formalin-induced LFP power in anesthetized animals, and (2) to assess the formalin-induced behavioral activity with ECT treatment in freely-moving animals. A portion of this data has been presented at the Society for Neuroscience (Trejo et al., 2023).

The power spectrum 5-minute data revealed mixed effects. Because we are better able to see the effects in the 10-second analyses, we believe that this is due to merging the various time points together in the 5-minute data, which may produce a washing out effect of the true nature

of the brief suppression of LFP power (Figure 11). The power spectrum 10-second analyses (Figures 12, 13, 14) first demonstrate the increase of LFP power post-formalin injection in all four designated brain regions (ACC, VTA, L-CeA, and R-CeA), further supporting the noxious effect of formalin (Figure 12). Secondly, in all four brain regions, the power spectrum 10-second data not only demonstrates the noxious escalating effect formalin possesses on LFP power, but this data also demonstrates the suppression of formalin-induced LFP power after receiving ECT stimulation (Figure 13). However, after analyzing the power spectrum data, we found that ECT does not exert long-lasting effects, but rather exhibits a brief suppressive effect. Formalin followed by ECT administration (group B) revealed a trend of brief inhibition of formalin-induced activity in all four brain regions, whereas ECT administration followed by formalin (group C) demonstrates a facilitatory effect (Figure 14). Due to the ECT administration followed by formalin (group C) condition not demonstrating as salient of an inhibitory LFP effect as the formalin followed by ECT administration (group B) condition, we lead to the conclusion that administering ECT after a pain-inducing event displays a trend that it may be the most effective.

In the behavioral testing conducted, animals received formalin injection and three ECT stimulations at 50mA for 2-seconds, results demonstrated a significant decrease between the 30 to 55min marks between groups when ECT is administered in comparison to the formalin-only group (Figure 6). These exciting results compare with other studies that demonstrate different methods for inducing analgesic effects in formalin-induced behavioral testing. As previously mentioned, it was revealed in one of the original formalin tests through behavioral testing, that morphine, meperidine, and PAG stimulation decreases formalin-induced pain in animal subjects. Moreover, electrical stimulation of the PAG after receiving formalin was comparable with animal subjects who received morphine and meperidine, and the authors even go on to suggest a

similarity in the mechanisms of the behavioral effects of PAG stimulation and morphine (Dubuisson & Dennis, 1977). Furthermore, in a separate study, it was revealed through behavioral testing that electrical stimulation of the cingulum bundle produces analgesia in stimulations administered both prior to and following formalin injections (Fuchs et al., 1996). These results demonstrate the different methods possible to inhibit formalin-induced pain through behavioral studies.

Perhaps the largest question that researchers face is, how does ECT actually work? The underlying mechanisms to understand exactly how ECT exerts its effects remains to be widely unknown, but there are various neurophysiological, neuro-biochemical, and neuroplasticity theories that many researchers have formed (Singh & Kar, 2017). A potential effect could be attributed to supraspinal mechanisms. These mechanisms demonstrate an influence upon circuitry of the brain by analgesics able to cross the blood-brain barrier and interact with the central nervous system (Bannister & Dickenson, 2020). With opioids, supraspinal effects act upon various structures such as the rostral ventral medulla (RVM), mesencephalic reticular formation (MRF), PAG, thalamus and cortex, and the limbic system (Jensen, 1997). ECT was shown to influence transmission of many neurotransmitters in the brain such as serotonin, dopamine, acetylcholine, and epinephrine, amongst others (Singh et al., 2017). More specifically, data reveals that ECT administration causes a change in glutamatergic neurotransmission, an increase of serotonergic and mesocorticolimbic dopaminergic neurotransmission, and lower GABA levels in specific structures (Stippl et al., 2020). Neurotransmitter release, receptor binding, and neurotransmission were levels at which the effects of ECT were revealed (Baldinger et al., 2014; Singh et al., 2017). These various changes point toward the possible supraspinal effect that ECT may exert.

For the current study, we hypothesized that the large seizure-inducing stimulation that travels across the brain could activate various brain areas, cortically, subcortically, and may even trigger the descending inhibitory system starting at the PAG, then moving to other structures such as the locus coeruleus (produces norepinephrine), the RMV which is in part composed of the nucleus raphe magnus (produces serotonin), and then descending to the spinal dorsal horn neurons to release neurotransmitters which causes a reduction of activity in projecting neurons in the spinal cord (Vanegas & Schaible, 2004; Trejo et al., 2023). In a study conducted by Senapati and colleagues (2005), the authors theorize that stimulation of the ACC activates PAG neurons, which ultimately activates the descending inhibitory system by spinal cord dorsal horn neurons. In conclusion, we lead with the theory that ECT suppresses formalin-induced LFP power and behavioral testing through activation of the descending inhibitory system.

Future research should determine the effect of ECT on the reduction of formalin-induced LFP power not only in anesthetized animals, but also in freely-moving animals. Additionally, there should be further testing to determine if there are inhibitory LFP effects in other models such as complete Freund's adjuvant (CFA) or carrageenan. Ultimately, this study has found promising data that supports the notion that ECT has pain-suppressing effects. Aside from ECT's long used history as a treatment for psychiatric disorders, the results from this study could have key components in the clinical implications for pain relief methods.

References

- Abdi, S., Haruo, A., & Bloomstone, J. (2004). Electroconvulsive Therapy for Neuropathic Pain
Electroconvulsive Therapy for Neuropathic Pain: A Case Report and Literature Review.
Pain Physician, 7(2), 261–263.
- Allen, H. N., Bobnar, H. J., & Kolber, B. J. (2021). Left and right hemispheric lateralization of
the amygdala in pain. *Progress in Neurobiology*, 196, 101891. doi:
10.1016/J.PNEUROBIO.2020.101891
- Antal, A., Brepohl, N., Poreisz, C., Boros, K., Csifcsak, G., & Paulus, W. (2008). Transcranial
direct current stimulation over somatosensory cortex decreases experimentally Induced
acute pain perception. *Clinical Journal of Pain*, 24(1), 56–63. doi:
10.1097/AJP.0b013e318157233b
- Antal, A., Kincses, T. Z., Nitsche, M. A., Bartfai, O., & Paulus, W. (2004). Excitability Changes
Induced in the Human Primary Visual Cortex by Transcranial Direct Current Stimulation:
Direct Electrophysiological Evidence. *Investigative Ophthalmology and Visual Science*,
45(2), 702–707. doi: 10.1167/iovs.03-0688
- Auvichayapat, P., Keeratitanont, K., Janyachareon, T., & Auvichayapat, N. (2018). The effects
of transcranial direct current stimulation on metabolite changes at the anterior cingulate
cortex in neuropathic pain: a pilot study. *Journal of Pain Research*, 11–2301. doi:
10.2147/JPR.S172920
- Badran, B. W., Caulfield, K. A., Stomberg-Firestein, S., Summers, P. M., Dowdle, L. T., Savoca,
M., Li, X., Austelle, C. W., Short, E. B., Borckardt, J. J., Spivak, N., Bystritsky, A., &
George, M. S. (2020). Sonication of the anterior thalamus with MRI-Guided transcranial

- focused ultrasound (tFUS) alters pain thresholds in healthy adults: A double-blind, sham-controlled study. *Brain Stimulation*, 13(6), 1805–1812. doi: 10.1016/j.brs.2020.10.007
- Baldinger P, Lotan A, Frey R, Kasper S, Lerer B, Lanzenberger R. Neurotransmitters and electroconvulsive therapy. *J ECT* 2014. doi: 30:116-121.
- Bannister, K., & Dickenson, A. H. (2020). *Central Nervous System Targets: Supraspinal Mechanisms of Analgesia*. doi: 10.1007/s13311-020-00887-6
- Berger, N. A., Besson, V. C., Boulares, A. H., Bürkle, A., Chiarugi, A., Clark, R. S., Curtin, N. J., Cuzzocrea, S., Dawson, T. M., Dawson, V. L., Haskó, G., Liaudet, L., Moroni, F., Pacher, P., Radermacher, P., Salzman, A. L., Snyder, S. H., Soriano, F. G., Strosznajder, R. P., ... Szabo, C. (2018). Opportunities for the repurposing of PARP inhibitors for the therapy of non-oncological diseases. In *British Journal of Pharmacology* (Vol. 175, Issue 2, pp. 192–222). John Wiley and Sons Inc. doi: 10.1111/bph.13748
- Bland, N. S., & Sale, M. v. (2019). Current challenges: the ups and downs of tACS. In *Experimental Brain Research* (Vol. 237, Issue 12, pp. 3071–3088). Springer. doi: 10.1007/s00221-019-05666-0
- Bonica, J. J. (1979). Editorial The need of a taxonomy. *PAIN*, 6(3), 247–252. doi: 10.1016/0304-3959(79)90046-0
- Busnello, J. V., Oses, J. P., da Silva, R. S., Feier, G., Barichello, T., Quevedo, J., Böhmer, A. E., Kapczinski, F., Souza, D. O., Sarkis, J. J. F., & Portela, L. V. (2008). Peripheral nucleotide hydrolysis in rats submitted to a model of electroconvulsive therapy. *Progress in Neuro-Psychopharmacology and Biological Psychiatry*, 32(8), 1829–1833. doi: 10.1016/j.pnpbp.2008.08.007

- Carr, D. B., & Sesack, S. R. (2000). *Projections from the Rat Prefrontal Cortex to the Ventral Tegmental Area: Target Specificity in the Synaptic Associations with Mesoaccumbens and Mesocortical Neurons.*
- Cohen, J. Y., Haesler, S., Vong, L., Lowell, B. B., & Uchida, N. (2012). *Neuron-type-specific signals for reward and punishment in the ventral tegmental area.* doi: 10.1038/nature10754
- Dubuisson, D., & Dennis, S. G. (1977). THE FORMALIN TEST: A QUANTITATIVE STUDY OF THE ANALGESIC EFFECTS OF MORPHINE, MEPERIDINE, AND BRAIN STEM STIMULATION IN RATS AND CATS. In *Pain* (Vol. 4). ElsevirrlNorth-Holland Biomedical Press.
- Esmailpour, Z., Marangolo, P., Hampstead, B. M., Bestmann, S., Galletta, E., Knotkova, H., & Bikson, M. (2018). Incomplete evidence that increasing current intensity of tDCS boosts outcomes. *Brain Stimulation, 11*(2), 310–321. doi: 10.1016/j.brs.2017.12.002
- Espinoza, R. T., & Kellner, C. H. (2022). Electroconvulsive Therapy. *New England Journal of Medicine, 386*(7), 667–672. doi: 10.1056/NEJMra2034954
- Fuchs, P. N., Balinsky, M., & Melzack, R. (1996). Electrical stimulation of the cingulum bundle and surrounding cortical tissue reduces formalin-test pain in the rat. In *Brain Research* (Vol. 743).
- Fuchs, P. N., Peng, Y. B., Boyette-Davis, J. A., & Uhelski, M. L. (2014). The anterior cingulate cortex and pain processing. In *Frontiers in Integrative Neuroscience* (Vol. 8, Issue MAY). Frontiers Research Foundation. doi: 10.3389/fnint.2014.00035

- Gandiga, P. C., Hummel, F. C., & Cohen, L. G. (2006). Transcranial DC stimulation (tDCS): A tool for double-blind sham-controlled clinical studies in brain stimulation. *Clinical Neurophysiology*, *117*(4), 845–850. doi: 10.1016/J.CLINPH.2005.12.003
- Goddard, G. v. (1964). FUNCTIONS OF THE AMYGDALA*. In *Psychological Bulletin* (Vol. 62, Issue 2).
- Halassa, M. M., Destexhe, A., Sohal, V. S., & Herreras, O. (2016). Local Field Potentials: Myths and Misunderstandings. *Frontiers in Neural Circuits / Www.Frontiersin.Org*, *10*, 101. doi: 10.3389/fncir.2016.00101
- Harris-Bozer, A. L., & Peng, Y. B. (2016). Inflammatory pain by carrageenan recruits low-frequency local field potential changes in the anterior cingulate cortex. *Neuroscience Letters*, *632*, 8–14. doi: 10.1016/j.neulet.2016.08.016
- Huang, Y. Z., Lu, M. K., Antal, A., Classen, J., Nitsche, M., Ziemann, U., Ridding, M., Hamada, M., Ugawa, Y., Jaberzadeh, S., Suppa, A., Paulus, W., & Rothwell, J. (2017). Plasticity induced by non-invasive transcranial brain stimulation: A position paper. In *Clinical Neurophysiology* (Vol. 128, Issue 11, pp. 2318–2329). Elsevier Ireland Ltd. doi: 10.1016/j.clinph.2017.09.007
- Jansson, L., Wennström, M., Johanson, A., & Tingström, A. (2009). Glial cell activation in response to electroconvulsive seizures. *Progress in Neuro-Psychopharmacology and Biological Psychiatry*, *33*(7), 1119–1128. doi: 10.1016/j.pnpbp.2009.06.007
- Jansson, L., Wennström, M., Tingström, A., Kyeremanteng, C., James, J., Merali, Z., Alftoa, A., Hinsley, T. A., Kõiv, K., Brass, A., & Harro, J. (2008). *Effect of stimulus parameters in a rat model of electroconvulsive seizures*. <http://ijnp.oxfordjournals.org/>

- Jensen, T. S. (1997). Opioids in the brain: Supraspinal mechanisms in pain control. *Acta Anaesthesiologica Scandinavica*, 41(1 II), 123–132. doi: 10.1111/j.1399-6576.1997.tb04626.x
- Johansen, J. P., Fields, H. L., Manning, B. H., & Kennedy, D. (2001). *The affective component of pain in rodents: Direct evidence for a contribution of the anterior cingulate cortex*. <https://www.pnas.org>
- Kalat, J. W. (2018). *Biological Psychology* (13th ed.). Cengage.
- Klein, M. M., Treister, R., Raij, T., Pascual-Leone, A., Park, L., Nurmikko, T., Lenz, F., Lefaucheur, J.-P., Lang, M., Hallett, M., Fox, M., Cudkowicz, M., Costello, A., Carr, D. B., Ayache, S. S., & Oaklander, A. L. (2015). *Transcranial magnetic stimulation of the brain: guidelines for pain treatment research*. doi: 10.1097/j.pain.0000000000000210
- LaGraize, S. C., & Fuchs, P. N. (2007). GABAA but not GABAB receptors in the rostral anterior cingulate cortex selectively modulate pain-induced escape/avoidance behavior. *Experimental Neurology*, 204(1), 182–194. doi: 10.1016/j.expneurol.2006.10.007
- Li, A. L., Sibi, J. E., Yang, X., Chiao, J. C., & Peng, Y. B. (2016). Stimulation of the ventral tegmental area increased nociceptive thresholds and decreased spinal dorsal horn neuronal activity in rat. *Experimental Brain Research*, 234(6), 1505–1514. doi: 10.1007/s00221-016-4558-z
- Loeser, J. D., & Melzack, R. (1999). *Pain: an overview*.
- Lozano, A. M., Lipsman, N., Bergman, H., Brown, P., Chabardes, S., Chang, J. W., Matthews, K., McIntyre, C. C., Schlaepfer, T. E., Schulder, M., Temel, Y., Volkmann, J., & Krauss, J.

- K. (2019). Deep brain stimulation: current challenges and future directions. In *Nature Reviews Neurology* (Vol. 15, Issue 3, pp. 148–160). Nature Publishing Group. doi: 10.1038/s41582-018-0128-2
- Marzbani, H., Marateb, H. R., & Mansourian, M. (2016). *Methodological Note: Neurofeedback: A Comprehensive Review on System Design, Methodology and Clinical Applications*. 7(2). doi: 10.15412/J.BCN.03070208
- Moret, B., Donato, R., Nucci, M., Cona, G., & Gianluca Campana, &. (2019). *transcranial random noise stimulation (tRnS): a wide range of frequencies is needed for increasing cortical excitability*. doi: 10.1038/s41598-019-51553-7
- Neugebauer, V. (2015). Amygdala pain mechanisms. *Handbook of Experimental Pharmacology*, 227, 261–284. doi: 10.1007/978-3-662-46450-2_13
- Neugebauer, V. (2020). Amygdala physiology in pain. In *Handbook of Behavioral Neuroscience* (Vol. 26, pp. 101–113). Elsevier B.V. doi: 10.1016/B978-0-12-815134-1.00004-0
- Neugebauer, V., Li, W., Bird, G. C., & Han, J. S. (2004). The amygdala and persistent pain. In *Neuroscientist* (Vol. 10, Issue 3, pp. 221–234). doi: 10.1177/1073858403261077
- Paulus, W. (2011). Transcranial electrical stimulation (tES - tDCS; tRNS, tACS) methods. *Neuropsychological Rehabilitation*, 21(5), 602–617. doi: 10.1080/09602011.2011.557292
- Paxinos, G., & Watson, C. (1997). *The rat brain, in stereotaxic coordinates*. Academic Press.
- Perrey, S., Teo, W.-P., Castelli, L., Brighina, F., Curatolo, M., Cosentino, G., de Tommaso, M., Battaglia, G., Sarzi-Puttini, P. C., Guggino, G., & Fierro, B. (2019). *Brain Modulation by*

Electric Currents in Fibromyalgia: A Structured Review on Non-invasive Approach With Transcranial Electrical Stimulation. doi: 10.3389/fnhum.2019.00040

Peterchev, A. v, Rosa, M. A., Deng, Z.-D., Prudic, J., & Lisanby, S. H. (2011). *ECT Stimulus Parameters: Rethinking Dosage.* doi: 10.1097/YCT.0b013e3181e48165

Raja, S. N., Carr, D. B., Cohen, M., Finnerup, N. B., Flor, H., Gibson, S., Keefe, F. J., Mogil, J. S., Ringkamp, M., Sluka, K. A., Song, X. J., Stevens, B., Sullivan, M. D., Tutelman, P. R., Ushida, T., & Vader, K. (2020). The revised International Association for the Study of Pain definition of pain: concepts, challenges, and compromises. In *Pain* (Vol. 161, Issue 9, pp. 1976–1982). Lippincott Williams and Wilkins. doi: 10.1097/j.pain.0000000000001939

Riedel, W., Neeck, G., & Kerckhoff, S. W. G. (2001). Nociception, pain, and antinociception: current concepts MAIN TOPIC. In *Z Rheumatol* (Vol. 60).

Russo, C. M., & Brose, W. G. (1998). Chronic pain. In *Annual Review of Medicine* (Issue 123). doi: 10.1146/annurev.med.49.1.123. PMID: 9509254.

Saiote, C., Turi, Z., Paulus, W., Antal, A., Miniussi, C., Herrmann, C. S., Baudewig, J., & Berlin, F. U. (2013). *Combining functional magnetic resonance imaging with transcranial electrical stimulation.* doi: 10.3389/fnhum.2013.00435

Salik, I., & Raman, M. (2022). *Electroconvulsive Therapy Continuing Education Activity.*

Senapati, A. K., Lagraize, S. C., Huntington, P. J., Wilson, H. D., Fuchs, P. N., & Peng, Y. B. (2005). Electrical stimulation of the anterior cingulate cortex reduces responses of rat dorsal horn neurons to mechanical stimuli. *Journal of Neurophysiology*, 94(1), 845–851. doi: 10.1152/jn.00040.2005

- Senba, E., & Kami, K. (2017). A new aspect of chronic pain as a lifestyle-related disease. In *Neurobiology of Pain* (Vol. 1, pp. 6–15). Elsevier B.V. doi: 10.1016/j.ynpai.2017.04.003
- Singh, A., & Kar, S. K. (2017). How electroconvulsive therapy works?: Understanding the neurobiological mechanisms. In *Clinical Psychopharmacology and Neuroscience* (Vol. 15, Issue 3, pp. 210–221). Korean College of Neuropsychopharmacology. doi: 10.9758/cpn.2017.15.3.210
- Stevens, F. L., Hurley, R. A., Taber, K. H., & Hayman, L. A. (2011). Anterior Cingulate Cortex: Unique Role in Cognition and Emotion WINDOWS TO THE BRAIN. In *J Neuropsychiatry Clin Neurosci* (Vol. 23, Issue 2). <http://neuro.psychiatryonline.org>
- Stippl, A., Kirkgöze, F. N., Bajbouj, M., & Grimm, S. (2020). Differential Effects of Electroconvulsive Therapy in the Treatment of Major Depressive Disorder. In *Neuropsychobiology* (Vol. 79, Issue 6, pp. 408–416). S. Karger AG. doi: 10.1159/000505553
- Suzuki, K., Ebina, Y., Shindo, T., Takano, T., Awata, S., & Matsuoka, H. (2009). *Repeated electroconvulsive therapy courses improved chronic regional pain with depression caused by failed back syndrome*. <http://www.medscimonit.com/abstract/index/idArt/869604>
- Świeboda, P., Filip, R., Prystupa, A., & Drozd, M. (2013). Assessment of pain: types, mechanism and treatment. In *Ann Agric Environ Med* (Vol. 1). www.aaem.pl
- Thompson, J. M., & Neugebauer, V. (2019). Cortico-limbic pain mechanisms. In *Neuroscience Letters* (Vol. 702, pp. 15–23). Elsevier Ireland Ltd. doi: 10.1016/j.neulet.2018.11.037

- Tjølsen, A., Berge, O. G., Hunskaar, S., Rosland, J. H., & Hole, K. (1992). The formalin test: an evaluation of the method. *Pain, 51*(1), 5–17. doi: 10.1016/0304-3959(92)90003-T
- Trejo, J., Wang, Z., Fuchs, P. N., Peng, Y. B. (2023) Exploratory study of the anti-nociceptive effect of electroconvulsive stimulation in rats. Society for Neuroscience
- Usui, C., Doi, N., Nishioka, M., Komatsu, H., Yamamoto, R., Ohkubo, T., Ishizuka, T., Shibata, N., Hatta, K., Miyazaki, H., Nishioka, K., & Arai, H. (2006). Electroconvulsive therapy improves severe pain associated with fibromyalgia. *Pain, 121*(3), 276–280. doi: 10.1016/j.pain.2005.12.025
- Vanegas, H., & Schaible, H. G. (2004). Descending control of persistent pain: Inhibitory or facilitatory? In *Brain Research Reviews* (Vol. 46, Issue 3, pp. 295–309). doi: 10.1016/j.brainresrev.2004.07.004
- Wang, Z., & Peng, Y. B. (2022). Multi-region local field potential signatures in response to the formalin-induced inflammatory stimulus in male rats. *Brain Research, 1778*. doi: 10.1016/j.brainres.2022.147779
- Woods, A. J., Antal, A., Bikson, M., Boggio, P. S., Brunoni, A. R., Celnik, P., Cohen, L. G., Fregni, F., Herrmann, C. S., Kappenman, E. S., Knotkova, H., Liebetanz, D., Miniussi, C., Miranda, P. C., Paulus, W., Priori, A., Reato, D., Stagg, C., Wenderoth, N., & Nitsche, M. A. (2016). A technical guide to tDCS, and related non-invasive brain stimulation tools. In *Clinical Neurophysiology* (Vol. 127, Issue 2, pp. 1031–1048). Elsevier Ireland Ltd. doi: 10.1016/j.clinph.2015.11.012

- Yu, K., Liu, C., Niu, X., & He, B. (2021). Transcranial Focused Ultrasound Neuromodulation of Voluntary Movement-Related Cortical Activity in Humans. *IEEE Transactions on Biomedical Engineering*, 68(6), 1923–1931. doi: 10.1109/TBME.2020.3030892
- Zhang, Q., Xiao, Z., Huang, C., Hu, S., Kulkarni, P., Martinez, E., Tong, A. P., Garg, A., Zhou, H., Chen, Z., & Wang, J. (2018). *Local field potential decoding of the onset and intensity of acute pain in rats OPEN*. doi: 10.1038/s41598-018-26527-w
- Zhang, T., Liang, H., Wang, Z., Qiu, C., Bo Peng, Y., Zhu, X., Li, J., Ge, X., Xu, J., Huang, X., Tong, J., Ou-Yang, J., Yang, X., Li, F., & Zhu, B. (2022). APPLIED SCIENCES AND ENGINEERING Piezoelectric ultrasound energy-harvesting device for deep brain stimulation and analgesia applications. In *Sci. Adv* (Vol. 8). <https://www.science.org>
- Zhang, T., Wang, Z., Liang, H., Wu, Z., Li, J., Ou-Yang, J., Yang, X., Peng, Y. B., & Zhu, B. (2022). Transcranial Focused Ultrasound Stimulation of Periaqueductal Gray for Analgesia. *IEEE Transactions on Biomedical Engineering*, 1–1. doi: 10.1109/tbme.2022.3162073